International Journal of Thermophysics, Vol. 26, No. 3, May 2005 (© 2005)
DOI: 10.1007/s10765-005-5567-5

Thermal Conductivity and Viscosity of Aqueous K_2SO_4 Solutions at Temperatures from 298 to 575 K and at Pressures up to 30 MPa

I. M. Abdulagatov[1–3] and N. D. Azizov[4]

Received September 15, 2004

The thermal conductivity of three (0.239, 0.499, and 0.782 mol·kg^{-1}) and the viscosity of four (0.0658, 0.2055, 0.3050, and 0.4070 mol·kg^{-1}) binary aqueous K_2SO_4 solutions have been measured with coaxial-cylinder (steady-state) and capillary-flow techniques, respectively. Measurements were made at pressures up to 30 MPa, and the range of temperature was 298–575 K. The total uncertainties of the thermal conductivity, viscosity, pressure, temperature, and composition measurements were estimated to be less than 2%, 1.6%, 0.05%, 30 mK, and 0.02%, respectively. The measured values of the thermal conductivity and viscosity of K_2SO_4 (aq) were compared with data and correlations reported in the literature. The reliability and accuracy of the experimental method was confirmed with measurements on pure water with well known (IAPWS standards) thermal conductivity and viscosity values (deviations, AAD, within 0.31 % and 0.52 %, respectively). The values of the viscosity *A*-, *B*-, and *D*-coefficients of the extended Jones–Dole equation for the relative viscosity (η/η_0) of aqueous K_2SO_4 solutions as a function of temperature were studied. The maximum of the *B*-coefficient near 340 K has been found. The derived values of the viscosity *A*- and *B*-coefficients were compared with results predicted by the Falkenhagen–Dole theory of electrolyte solutions and calculated with the ionic *B*-coefficient data. The behavior of the concentration dependence of the relative viscosity of aqueous K_2SO_4 solutions is discussed in terms of the modern theory of transport phenomena in electrolyte solutions.

[1]Institute for Geothermal Problems of the Dagestan Scientific Center of the Russian Academy of Sciences, Shamilya Str. 39-A, 367003 Makhachkala, Dagestan, Russia.
[2]Present address: Physical and Chemical Properties Division, National Institute of Standards and Technology, 325 Broadway, Boulder, Colorado 80305, U.S.A.
[3]To whom correspondence should be addressed. E-mail: ilmutdin@boulder.nist.gov
[4]Azerbaijan State Oil Academy, Baku 370601, Azerbaijan.

KEY WORDS: aqueous solution; capillary viscometer; coaxial-cylinder technique; potassium sulfate; thermal conductivity; *B*-coefficient; viscosity; water.

1. INTRODUCTION

The transport properties (thermal conductivity and viscosity) of aqueous solutions are important in many industrial processes such as material transport, solid deposition, corrosion in steam generators, and electrical power boilers [1]. Knowledge of the pressure, temperature, and composition dependences of transport properties of aqueous electrolyte solutions are essential to understand a variety of problems in a number of technological and engineering applications as follows: chemical processes, desalination processes, geochemistry (hydrothermal formation of minerals, growth of K_2SO_4 crystals from aqueous solutions [2, 3]), calculation of design parameters, development and utilization of geothermal and ocean thermal energy, geology and mineralogy, prediction of heat- and mass-transfer coefficients, environmental applications, and treatment of wastewater. To understand and control those processes that use electrolyte solutions, it is necessary to know their thermodynamic and transport properties.

The thermal conductivity and viscosity of electrolyte solutions are also of research interest (scientific applications) because the long-range electrostatic interactions (coulombic forces between ions) cause difficulty in describing the behavior of such systems [4–11]. Electrostatic interactions govern thermodynamic and transport properties of ionic electrolyte solutions. Available theoretical models frequently cannot describe real systems as they are met in practice (for example, complex ionic solutions are extremely difficult). Better predictive models can be developed based on reliable experimental information on thermodynamic and transport properties. However, measurements of the thermal conductivity and viscosity of aqueous salt solutions have so far been limited to rather narrow ranges of temperature, pressure, and concentration with less than satisfactory accuracy.

Thermal conductivity data of $H_2O + K_2SO_4$ solutions are extremely scarce. The reported thermal conductivity data [12–15] are at low temperatures (at 293 K) and at atmospheric pressure. A literature survey revealed that there are no thermal conductivity data for $H_2O + K_2SO_4$ solutions under pressure and at high temperatures. Previously, viscosity data of $H_2O + K_2SO_4$ solutions have been reported by several authors [16–28]. All measurements, except those of Correia and Kestin [17], were performed at atmospheric pressure.

The main objective of the paper is to provide new accurate experimental thermal conductivity and viscosity data for binary $H_2O + K_2SO_4$ solutions at high temperatures (up to 575 K) and high pressures (up to 30 MPa) for compositions up to 0.782 mol·kg^{-1} using coaxial-cylinder (steady-state) and capillary-flow techniques, respectively, which have been previously used for accurate measurements on other systems at high temperatures and high pressures [29–47]. The present results expand considerably the temperature, pressure, and concentration ranges for which thermal conductivity and viscosity data for aqueous K_2SO_4 solutions are available. This work is a part of a continuing program on the transport properties (thermal conductivity and viscosity) of electrolytes in aqueous solutions at high temperatures and high pressures. In previous studies [29–47] we measured the thermal conductivity and viscosity of 30 aqueous salt solutions at high temperatures (up to 573.15 K) and high pressures (up to 100 MPa) using coaxial-cylinder, parallel-plate, and capillary-flow techniques.

2. LITERATURE REVIEW OF EXPERIMENTAL THERMAL CONDUCTIVITY AND VISCOSITY DATA, CORRELATIONS, AND THEORETICAL MODELS FOR $H_2O + K_2SO_4$ SOLUTIONS

2.1. Thermal Conductivity Experimental Data and Correlations

Vernigora et al. [12] employed the coaxial-cylinder technique (relative version) to measure the thermal conductivity of aqueous K_2SO_4 solutions in the temperature range from 293.15 to 363.15 K and at atmospheric pressure for concentrations between 2 and 14 mass%. The uncertainty of the measurements is 1–2%.

Vargaftik and Os'minin [13] reported one value of the thermal conductivity of aqueous K_2SO_4 solutions at a temperature of 293.15 K and a concentration of 10 mass% and at atmospheric pressure. To calculate the thermal conductivity of dilute aqueous solutions at high temperatures, Vargaftik and Os'minin [13] recommended the following relationship:

$$\lambda_{sol}(T) = \left[\frac{\lambda_0(T)}{\lambda_0(293)}\right] \lambda_{sol}(293), \tag{1}$$

where $\lambda_0(293) = 598.5\ \text{mW·m}^{-1}\text{·K}^{-1}$ and $\lambda_0(T)$ is the thermal conductivity of pure water. As one can see from this equation, the ratio between the thermal conductivity at 293 K and at temperature T is colinear with that of pure water. This equation described the temperature dependence of aqueous salt solutions within 1–2% at temperatures up to 373 K.

Riedel [14] also measured the thermal conductivity of aqueous K_2SO_4 solutions at a temperature of 293.15 K and at atmospheric pressure for

two concentrations, 5 and 10 mass%. He proposed a correlation equation for the thermal conductivity of aqueous solution using the ionic contribution technique;

$$\lambda_{sol} = \lambda_0 + \sum_i \alpha_i c_i, \tag{2}$$

where $\alpha_+(K^+) = -0.0065$, $\alpha_-(SO_4^{-2}) = 0.001$, and c is the concentration in $mol \cdot L^{-1}$.

Aseyev [48] expressed available experimental thermal conductivity data from the literature for binary and ternary aqueous salt solutions by the equation,

$$\lambda = \lambda_0 \left(1 + \sum_{i=1} \beta_i x_i\right), \tag{3}$$

where λ_0 is the thermal conductivity of pure water in $W \cdot m^{-1} \cdot K^{-1}$ and x is the concentration in mass%. The value of the coefficient β_i in Eq. (3) for K_2SO_4 solutions is $\beta_i = -0.0009591$. This equation is valid in the temperature range from 273 to 373 K and at concentrations up to 16 mass%. The absolute uncertainty of the calculated values of the thermal conductivity of $H_2O + K_2SO_4$ is 0.00238 $W \cdot m^{-1} \cdot K^{-1}$.

Abdulagatov and Magomedov [29–39] developed a correlation equation to describe the thermal conductivity of aqueous salt solutions at high temperatures and high pressures,

$$\lambda_{sol}(T, P, x) = \lambda_0(P, T)\left\lfloor 1 - A(x + 2 \times 10^{-4} x^3)\right\rfloor - 2 \times 10^{-8} PTx, \tag{4}$$
$$\lambda_0(P, T) = 7 \times 10^{-9} T^3 - 1.511 \times 10^{-5} T^2 + 8.802 \times 10^{-3} T - 0.8624 + 1.6 \times 10^{-6} PT,$$

where $\lambda_{sol}(T, P, x)$ is the thermal conductivity of the solution in $W \cdot m^{-1} \cdot K^{-1}$, $\lambda_0(P, T)$ is the thermal conductivity of pure water in $W \cdot m^{-1} \cdot K^{-1}$, x is the concentration in mass%, T is the temperature in K, P is the pressure in MPa, and A is an adjustable parameter. The value of the coefficient A in Eq. (4) for $H_2O + K_2SO_4$ solutions is 0.00141 [49]. In the limit $x \to 0$, the thermal conductivity of pure water $\lambda_0(P, T)$ is obtained from Eq. (4). This equation is applicable in the temperature range from 273 to 473 K, at pressures up to 100 MPa, and at concentrations between 0 and 25 mass%, although some reasonable extrapolation to higher concentrations is possible.

DiGuilio et al. [50], DiGuilio and Teja [51], and Bleazard et al. [52, 53] were able to extend the pressure range by multiplying the thermal conductivity of salt solutions λ_{sol} at atmospheric pressure ($P = 0.1$ MPa) by

the ratio of the thermal conductivity of water at the desired pressure $\lambda_0(P)$ to that of water at $P = 0.1$ MPa;

$$\lambda_{sol}(P) = \left[\frac{\lambda_0(P)}{\lambda_0(0.1)}\right]\lambda_{sol}(0.1), \tag{5}$$

where $\lambda_0(0.1)$ is the thermal conductivity of pure water at $P = 0.1$ MPa and a given temperature, in $mW \cdot m^{-1} \cdot K^{-1}$, $\lambda_0(P)$ is the thermal conductivity of pure water at the desired pressure and the given temperature, and $\lambda_{sol}(0.1)$ is the thermal conductivity of the solution at atmospheric pressure and the given temperature.

2.2. Viscosity Experimental Data and Correlations

A literature survey revealed that all previous reported viscosity data for aqueous K_2SO_4 solutions were performed at atmospheric pressure, except for the data reported by Correia and Kestin [17]. A brief analysis of the different data sets is given below.

Puchkov and Sargaev [18] reported viscosity data for aqueous K_2SO_4 solutions at pressures slightly above the vapor pressure (0.1–2 MPa), at temperatures from 298 to 473 K, and at concentrations between 0.177 and 0.637 $mol \cdot kg^{-1}$. Measurements were made with the falling-body method. The uncertainty in the viscosity measurements is about 3%. Maksimova et al. [19] reported viscosity data for $H_2O + K_2SO_4$ solutions from 293 to 363 K for compositions between 0.058 and 0.6376 $mol \cdot kg^{-1}$at atmospheric pressure. Measurements were performed by means of a capillary method with an uncertainty of 0.5 %. Chesnokov [20] measured the kinematic viscosities of K_2SO_4 (aq) at 293.15 K and at two concentrations, 0.25 and 0.5 $mol \cdot L^{-1}$.

Correia and Kestin [17] reported experimental data for the viscosity of aqueous K_2SO_4 solutions in the pressure range from 0.1 to 31 MPa and the temperature range from 292.65 to 362.65 K. Measurements were performed with an oscillating-disk viscometer. The measurements cover the concentration range from 0.1491 to 0.5998 $mol \cdot kg^{-1}$. The experimental viscosity results have an estimated uncertainty of 1.0 %. A linear function of pressure along an isotherm was used to correlate measured values of the viscosity of K_2SO_4 (aq);

$$\eta(P, t, c) = \eta_0(T, c)\,[1 + \beta(T, c)P], \tag{6}$$

where $\eta_0(T, c)$ and $\beta(T, c)$, the hypothetical zero-pressure viscosity and pressure coefficients, respectively, were correlated in term of temperature and concentration.

Kaminsky [21] measured the viscosities of dilute (from 0.0025 to 0.0900 m) aqueous K_2SO_4 solutions from 285.65 to 315.65 K and at atmospheric pressure. The results of the measurements were used to calculate the viscosity A-, B-, and D-coefficients in the extended Jones–Dole equation. Jones and Colvin [22] reported relative viscosity data and the values of A- and B-coefficients for $H_2O + K_2SO_4$ solutions at 273.15 and 298.15 K at concentration from 0.0005 to 0.30138 mol·l^{-1}. Tanaka [25] reported relative viscosity data for $H_2O + K_2SO_4$ solutions from 283 to 333 K and for compositions between 0.1 to 0.9 mol·kg^{-1}. Ishii and Fujita [28] measured the viscosity of concentrated $H_2O + K_2SO_4$ solutions using an Ostwald viscometer at temperatures from 298 to 333 K.

Zaytsev and Aseyev [16] represented available experimental viscosity data for $H_2O + K_2SO_4$ solutions from the literature by the following correlation equation:

$$\log_{10}\eta = \log_{10}\eta_0 + 10^{-2}(0.457 + 0.00491T)x, \tag{7}$$

where η_0 is the viscosity of pure water (in mPa·s), x is the composition (in mass%), and T is the temperature (in °C). The absolute uncertainty of the calculated values of the viscosity of H_2O + K_2SO_4 is 0.0888 Pa·s.

2.3. Theoretical Models

Jiang and Sandler [6] developed a new statistical mechanics-based model for the viscosity of electrolyte solutions. This model is based on the combination of liquid-state theory and absolute-rate theory;

$$\frac{\eta}{\eta_0} = (1 + a\sqrt{c} + bc)\exp(f_{EX}/(RT)), \tag{8}$$

where f_{EX} is the excess contribution of the activation Helmholtz energy of the solution with the pure solvent. Jiang and Sandler [6] provided an analytical expression for hard-sphere and electrostatic contributions $f_{EX} = f_{HS} + f_{EL}$. The parameters a and b in Eq. (8) have physical meaning. As is the case for the parameter B in the Jones–Dole equation (see Section 4.2, Eq. (14)), the b value indicates the degree of order or disorder introduced by ions into the solvent structure. There are four parameters in this model $(a, b, \sigma_1^+, \varepsilon_1)$, where σ_1^+ and ε_1 are the ion diameter (hydration effect) and dielectric constant parameter (polarization effect), respectively. For most aqueous electrolyte solutions the value of a is close to 1.6. Therefore, the parameter a can be assigned a common value of 1.6 without losing accuracy in describing experimental viscosity data.

Esteves et al. [7] developed a new model for correlating the viscosity of binary strong electrolyte solutions. The proposed model is based on

Eyring's absolute rate theory and the Debye–Hückel model for calculating the excess (electrostatic) free energy of activation of the viscous flow. According to this model, the relative viscosity of binary aqueous solutions can be written as follows [7]:

$$\frac{\eta}{\eta_0} = 1 + A(c_1 + c_2)\exp[(\Psi_E^{DH} + \Psi_E^{G})/(RT)], \tag{9}$$

where c_1 and c_2 are the molar concentrations of the solute species; Ψ_E^{DH} and Ψ_E^{G} are the excess free energies of the electrolyte solution due to electrostatic (long-range) interactions of the ionic species (Debye–Hückel model) and the Guggenheim correction of the Debye–Hückel model, respectively. This model contains two empirical adjustable parameters (A and B). This model was used to correlate available experimental viscosity data for $H_2O + K_2SO_4$ solutions at 298.15 K and 0.1 MPa in the concentration range of 0.0005 to 0.5 m. The derived values of the adjustable parameters A and B for $H_2O + K_2SO_4$ solutions are 0.1316 and 0.2163, respectively. The overall average mean relative standard deviation (MRSD) is 0.03 %. The same data were fitted to the Jones–Dole model (see Eq. (14), Section 4.2) with MRSD of 0.49 %.

Lencka et al. [11] developed a comprehensive model for calculating the viscosity of aqueous electrolyte solutions ranging from dilute to very concentrated. The model includes a long-range electrostatic interactions term, η_r^{LR}, (Onsager-Fuss theory), contributions of individual ions, η_r^{S}, (using Jones–Dole B-coefficients), and a contribution of specific interactions between ions or neutral species, η_r^{S-S}, (for the concentrated solutions, function of the ionic strength);

$$\frac{\eta}{\eta_0} = 1 + \eta_r^{LR} + \eta_r^{S} + \eta_r^{S-S}. \tag{10}$$

A technique for predicting the temperature dependence of the viscosity B-coefficients has been developed using the concept of structure-breaking and structure-making ions;

$$B = B_E + B_S \exp[-K(T - 273.15)], \tag{11}$$

where $K = 0.023$ is a constant; $B_E = 0.365936\ \mathrm{L{\cdot}mol^{-1}}$ is the Einstein contribution (hydrodynamic, intrinsic term); and $B_S = -0.303513\ \mathrm{L{\cdot}mol^{-1}}$. The model reproduces the viscosity of aqueous systems ranging from dilute to concentrated solutions (30 m) at temperatures up to 573 K.

Chandra and Bagchi [8, 9] developed a new microscopic model for the ionic contribution to the viscosity of dilute electrolyte solutions on the basis of mode coupling theory. They presented a microscopic study of

the concentration dependence of the viscosity of an electrolyte solution. According to this theory at finite concentration, the viscosity increases nonlinearly with the square root of concentration ($\eta/\eta_0 \propto \sqrt{c}$) contrary to the Falkenhagen [63] equation. This model correctly reduces to the Falkenhagen expression [63] of reduced viscosity ($\eta/\eta_0 \propto \sqrt{c}$) at very low concentrations ($c \to 0$). Numerical calculations reveal that at a finite concentration the viscosity of a solution can be very different than that given by the Falkenhagen expression [63]. This theory predicts a stronger increase of viscosity with concentration than the classical theory of Falkenhagen [63]. At a finite concentration, the viscosity increases nonlinearly with the square root of the concentration, contrary to the linear increase predicted by the Falkenhagen theory [63].

3. EXPERIMENTAL APPARATUS AND PROCEDURES

3.1. Thermal Conductivity Measurements

The thermal conductivity of binary $H_2O + K_2SO_4$ solutions was measured with a coaxial-cylinder (steady-state) technique. The experimental apparatus used in this work is the same as was previously employed for the measurement of $H_2O + Li_2SO_4$, $Zn(NO_3)_2$, $Ca(NO_3)_2$, $Mg(NO_3)_2$, $Sr(NO_3)_2$, KBr, NaBr, and $LiNO_3$ solutions [40–42]. The apparatus and procedures that were described previously [40–42] were used without modification. Only a brief discussion will be given here. The main part of the apparatus consisted of a high-pressure autoclave, thermostat, and thermal-conductivity cell. The thermal-conductivity cell consisted of two coaxial cylinders: the inner (emitting) cylinder and the outer (receiving) cylinder. The cylinders were located in a high-pressure autoclave. The deviation from concentricity was less than 0.002 cm or 2% of the sample layer.

The autoclave was located in a thermostat. The thermostat was a solid (massive) copper block. The temperature in the thermostat was controlled with a heater. The thermostat is supplied with three sectioned heating elements, a PRT-10, and three chromel–alumel thermocouples that were located on three different levels of the copper block. The temperature differences between various sections (levels) of the copper block were within 0.02 K. The temperature was measured with a PRT and with three chromel-alumel thermocouples. The thermocouples were used to minimize the temperature gradients. The thermocouples were twice calibrated with a standard resistance thermometer, and the difference between the calibrations was 10 mK.

The solution under investigation is confined in the vertical gap of the cell. The pressure in the system was generated and measured with piston

manometers with upper limits of measurement of 60 and 600 bar. In the cell, heat was generated in the micro-heater, which consists of an isolated (high-temperature lacquer-covered) constantan wire of 0.1 mm diameter. A micro-heater was mounted inside the inner cylinder (emitter) which was wound closely around a surface of a 2 mm diameter ceramic tube and insulated with high temperature lacquer.

With this method the heat generated in an inner emitting cylinder is conducted radially through the narrow fluid-filled annulus to a coaxial receiving cylinder. The thermal conductivity λ of the fluid was deduced from measurements of the heat Q transmitted across the solution layer, the temperature difference ΔT between the inner and outer cylinders, the thickness of the solution layer d, and the effective length l of the measuring part of the cylinder (effective length of the cylinders). After taken all corrections into account, the final working equation for the thermal conductivity can be written as [40]

$$\lambda = A \frac{Q_{\text{meas}} - Q_{\text{los}}}{\Delta T_{\text{meas}} - \Delta T_{\text{corr}}}, \tag{12}$$

where $A = \ln\left(\frac{d_2}{d_1}\right)/(2\pi l)$ is the geometric constant which can be determined from geometrical characteristics of the experimental cell; Q_{meas} is the amount of heat released by the calorimetric micro-heater; Q_{los} is the amount of heat losses through the ends of the measuring cell (end effect); $\Delta T_{\text{corr}} = \Delta T_{\text{cl}} + \Delta T_{\text{lac}}$; ΔT_{cl} and ΔT_{lac} are the temperature differences in the cylinder walls and lacquer coat, respectively; and ΔT_{meas} is the temperature difference measured with differential thermocouples. The values of A can also be determined by means of a calibration technique using thermal conductivity data for the reference fluid (pure water, [54]). The values of the cell constant determined from geometrical characteristics of the experimental cell and by calibration techniques (pure water at temperature 293.15 K) are 0.1727 and 0.1752 m^{-1}, respectively. In this work we used the value of A as a function of temperature derived using the calibration procedure with pure water [54]. The geometrical constant A changes by 12% over the temperature range from 293.15 to 750.15 K. The change in the cell size due to pressure was considered negligible due to the low volume compressibility of stainless steel (1X18H9T). As one can see from Eq. (12), the propagation of uncertainty related to the difference between calculated and calibrated values of the geometric constant A is about 1.4%.

Due to the large emitter size and the small fluid volume surrounding the emitter, no effect of accommodation was to be expected. The calibration of the cell was made at a pressure of 60 MPa to avoid corrections due to the accommodation effect.

It is difficult to estimate the values of Q_{los} and ΔT_{corr} by calculation. In this work the values of Q_{los} and ΔT_{corr} were estimated by measuring a standard liquid (water) with a well known thermal conductivity (IAPWS [54] standard). The calibration was made with pure water at 10 selected temperatures between 293.15 and 713.15 K and at three selected pressures between 0.1 and 60 MPa. The amount of heat flow Q and the temperature difference ΔT were 13.06 W and 3.5 K, respectively. The estimated value of Q_{los} is about 0.05 W. This value is negligible (0.38%) by comparison with the heat transfer by conduction $Q = 13.06$ W.

To reduce the values of the Rayleigh number, Ra, a small gap distance between cylinders $d = (0.97 \pm 0.03) \times 10^{-3}$ m was used. This makes it possible to minimize the risk of convection. Convection could develop when the Ra exceeds a certain critical value Ra_c, which for vertical coaxial cylinders is about 1000 [55]. Therefore, $Ra > 1000$ was considered as a criterion for the beginning of convection. In the range of the present experiments, the values of Ra were always less than 500 and Q_{con} was estimated to be negligibly small. The absence of convection can be verified experimentally by measuring the thermal conductivity with different temperature differences ΔT across the measurement gap and different powers Q transferred from the inner-to-outer cylinder. The measured thermal conductivity was indeed independent of the applied temperature differences ΔT and power Q transferred from the inner to outer cylinder.

Any conductive heat transfer must be accompanied by simultaneous radiative transfer. The correction depends upon whether or not the fluid absorbs radiation. The inner and outer cylinders were perfectly polished with powder of successively smaller grain size (320 nm); their emissivity ($\varepsilon = 0.32$) was small; and the heat flux arising from radiation Q_{rad} is negligible by comparison with the heat transfer by conduction in the temperature range of our experiment. To minimize the heat transfer by radiation, a solid material (stainless-steel 1X18H9T) of low emissivity was used for the cylinders and thin layers of fluid (from 0.97 mm) are employed. In this way heat transport by radiation can be strongly reduced compared to the heat transport by conduction. The correction for absorption is small for pure water and for aqueous solutions in the temperature range up to 600 K, and we assumed it was negligible. Its influence on the uncertainty of the thermal conductivity is relatively small. The emissivity of the walls was small, and Q_{rad} is negligible (≈ 0.164 W) by comparison with the heat transfer (13.06 W) by conduction in the temperature range of our experiment.

The uncertainty analysis was carried out similarly as in previous studies [40–42]. Measurement uncertainties are associated with uncertainties in measured quantities contained in working Eq. (12) used to compute the

thermal conductivity from experimental data. The thermal conductivity was obtained from the measured quantities A, Q, T, ΔT, P, and x. As the uncertainties of the measured values d_1, d_2, and l are 0.15%, 0.09%, and 0.07%, respectively, the corresponding uncertainty of A is 0.5%. The experimental uncertainty in the concentration is estimated to be 0.02%. The uncertainty of the temperature and pressure measurements are $\theta_T = 0.02\,\mathrm{K}$ and $\theta_P = 0.03\,\mathrm{MPa}$ at pressures to 60 MPa. The corresponding uncertainty of the thermal conductivity measurement associated with uncertainties of temperature and pressure measurements is estimated to be less than 0.006%. The uncertainty in heat flow Q measurement is about 0.1%. To make sure that the cell was at equilibrium, measurements were started ten hours after the time when the thermostat temperature reached the targeted temperature. About five to six measurements are carried out at one state, and the average value of thermal conductivity is calculated. The reproducibility (scatter of the different measurements) of the measurements is about 0.5%. From the uncertainty of the measured quantities and the corrections mentioned above, the total maximum relative uncertainty $\delta\lambda/\lambda$ in the thermal conductivity is estimated to be 2%.

To check and confirm the uncertainty of the method and procedure of the measurements, thermal conductivity data were taken for pure water in the temperature range from 290.6 to 575.4 K at pressures up to 40 MPa. Table I provides the present experimental thermal conductivity data for pure water measured using the same experimental apparatus. Figure 1

Table I. Experimental Thermal Conductivities of Pure Water as a Function of Pressure and Temperature

	$\lambda\,(\mathrm{W\cdot m^{-1}\cdot K^{-1}})$		
T (K)	0.1 MPa	10 MPa	30 MPa
298.3	0.607	0.613	0.623
313.1	0.629	0.634	0.644
333.3	0.651	0.656	0.666
352.9	0.667	0.672	0.682
363.4	0.673	0.678	0.689
393.1	–	0.689	0.702
423.3	–	0.691	0.704
448.7	–	0.685	0.699
474.3	–	0.672	0.689
499.3	–	0.652	0.672
523.4	–	0.624	0.649
548.4	–	0.591	0.622
573.5	–	0.547	0.588

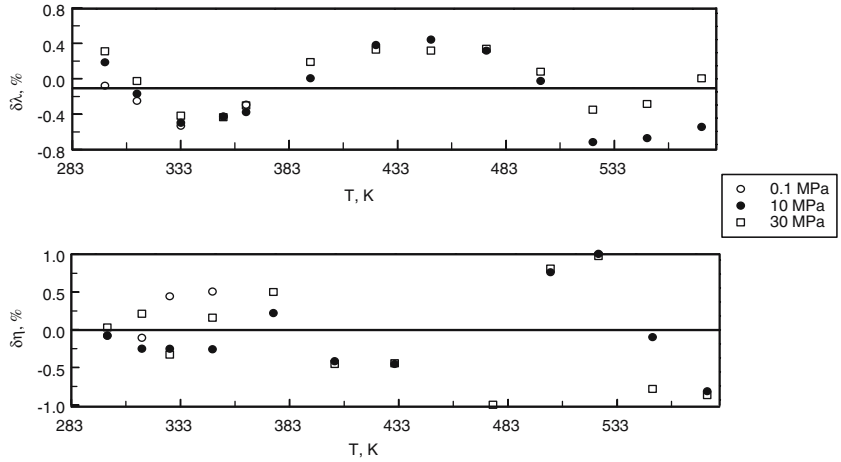

Fig. 1. Thermal conductivity, $\delta\lambda = 100(\lambda_{exp} - \lambda_{cal})/\lambda_{exp}$, and viscosity, $\delta\eta = 100(\eta_{exp} - \eta_{cal})/\eta_{exp}$, deviations of the experimental data for pure H_2O from values calculated with IAPWS [54] formulation.

provides detailed comparisons of the present test measurements for pure water with the reference data for water [54]. Figure 1 shows that the agreement between test measurements for pure water and IAPWS [54] calculations is excellent; deviation statistics are: AAD = 0.31, Bias = −0.13, St. Dev = 0.35, Std. Err = 0.06, and Max Dev = 0.72%. Excellent agreement is also found between present thermal conductivity results for pure water and the data reported by other authors (AAD within 0.2 to 0.67 %) and reference data reported by Ramires et al. [56] (AAD = 0.3%). This excellent agreement for test measurements demonstrates the reliability and accuracy of the present thermal conductivity measurements for binary $H_2O + K_2SO_4$ solutions (Table II).

3.2. Viscosity Measurements

The apparatus and procedures used for the viscosity measurements of the $H_2O + K_2SO_4$ solutions have been described in detail in previous papers [43–47] and were used without modification. Only brief and essential information will be given here. The measurements were made using a capillary-flow method which gives an uncertainty of 1.5%. The main parts of the apparatus consisted of a working capillary with an extension tube, a high-temperature and high-pressure autoclave, movable and unmovable cylinders, electrical heaters, and a solid red copper block. The

Table II. Experimental Thermal Conductivities ($W \cdot m^{-1} \cdot K^{-1}$) of $H_2O + K_2SO_4$ Solutions as a Function of Pressure, Temperature, and Concentration

T(K)	0.1 MPa	10 MPa	30 MPa
$m = 0.239\ mol \cdot kg^{-1}$			
298.4	0.605	0.610	0.620
313.0	0.626	0.631	0.641
333.6	0.649	0.654	0.664
353.3	0.665	0.670	0.679
363.4	0.670	0.675	0.685
393.5	–	0.684	0.695
423.6	–	0.683	0.696
448.7	–	0.678	0.691
473.4	–	0.665	0.681
498.5	–	0.644	0.664
523.3	–	0.617	0.637
547.9	–	0.584	0.610
573.8	–	0.540	0.574
$m = 0.499\ mol \cdot kg^{-1}$			
298.0	0.602	0.607	0.616
313.6	0.622	0.627	0.637
333.7	0.645	0.650	0.660
352.9	0.660	0.665	0.675
363.0	0.666	0.671	0.680
393.1	–	0.679	0.690
423.0	–	0.678	0.690
449.8	–	0.672	0.686
472.9	–	0.659	0.676
498.3	–	0.639	0.657
523.2	–	0.610	0.630
548.2	–	0.577	0.604
573.2	–	0.534	0.568
$m = 0.782\ mol \cdot kg^{-1}$			
313.1	0.618	0.623	0.632
333.3	0.640	0.645	0.655
352.9	0.654	0.659	0.670
363.4	0.660	0.665	0.675
393.1	–	0.672	0.685
423.3	–	0.671	0.684
448.1	–	0.665	0.681
473.8	–	0.652	0.671
498.6	–	0.632	0.650
523.9	–	0.602	0.623
548.5	–	0.570	0.598
573.2	–	0.525	0.560

capillary together with an extension tube were located in the high-temperature and high-pressure autoclave. When the movable cylinder was moved vertically at constant speed, the fluid flowed through the capillary. The autoclave was placed in a solid red copper block. Two electrical heaters were wound around the surface of the copper block. To generate and measure the pressure, the autoclave was connected to a dead-weight pressure gauge (MP-600) by means of a separating vessel. The uncertainty in pressure measurements was 0.05%.

The final working equations for this method are [43]

$$\eta = U\tau\frac{\rho}{\rho_c}\left(1-\frac{\rho_c}{\rho_{Hg}}\right)(1+\alpha\Delta T)^3 - W\frac{\rho_c}{\tau}, \quad U=\frac{g\pi R^4\Delta H_0\rho_{0,Hg}}{8LV_C} \text{ and } W=\frac{mV_c}{8\pi L}, \tag{13}$$

where $R = 0.15091$ mm is the inner radius of the capillary, $L = (540.324 \pm 0.005)$ mm is the capillary tube length, τ is the time of flow, α is the linear expansion coefficient of the capillary material, ΔT is the temperature difference between the experimental temperature and room temperature, $m = 1.12$ is a constant, $\rho(P, T)$ is the density of the fluid under study at the experimental conditions (P,T), $V_C = 1.2182\,\text{cm}^3$ is the volume of the unmovable (measuring) cylinder, ρ_C is the density of the fluid under study at room temperature and experimental pressure, $\Delta H_0 = (H_1 - H_2)/\ln(H_1/H_2)$, where H_1 and H_2 are the mercury levels at the beginning and end of the flowing fluid, respectively, at room temperature and atmospheric pressure, ρ_{Hg} is the density of mercury at room temperature and experimental pressure, and $\rho_{0,Hg}$ is the density of mercury at room temperature and atmospheric pressure. Equation (13) was derived from Poisseuille's law with corrections for the temperature effects on the capillary sizes and mercury and sample densities at the experimental conditions (P, T), and for the entrance effects (acceleration of a fluid at the inlet and outlet) on the fluid [43].

The values of the parameters U and W can also be determined by means of a calibration technique. The values of the capillary radius determined with both weighing and by calibration techniques are 0.15091 and 0.15048 mm, respectively. In this work we used the value of 0.15091 mm. The time of fluid flow through the capillary τ was measured with a stopwatch with an uncertainty of less than 0.1 s (0.5%). An electromagnetic device was used to start and stop the watch.

The viscosity was obtained from the measured quantities R^4, ΔH_0, L, V_C, τ, ρ_{Hg}, ρ_C, T, P, and m. The uncertainty of the viscosity measurements was assessed by analyzing the sensitivity of Eq. (13) to the experimental uncertainties of the measured quantities. At the maximum measured temperature (573 K), the value of the root-mean-square deviations in the

viscosity measurements was $\delta\eta = 2 \times 10^{-5}$ g·cm^{-1}·s^{-1}. Based on a detailed analysis of all sources of uncertainties likely to affect the determination of viscosity with the present apparatus, the combined maximum relative uncertainty $\delta\eta/\eta$ in measuring the viscosity was 1.5 % (see Abdulagatov and Azizov [43]). The Reynolds (Re) number for all measurements was less than the critical value ($Re_c = 300$).

As one can see from Eq. (13), to calculate the dynamic viscosity from measured quantities, the values of the density of the solution under study at room temperature and experimental pressure ρ_C, and the density at the experimental conditions $\rho(P, T)$ are needed. For this goal we used the density data reported in our previous publications [57, 58] for aqueous K_2SO_4 solutions at high temperatures (up to 573 K) and high pressures (up to 40 MPa).

As a check of the method and procedure of the measurements, the viscosity of pure water was measured from 299.76 to 574.54 K along three isobars (0.1, 10, and 30) MPa. Table III provides the present experimental viscosity data for pure water measured using the same experimental apparatus. These data were compared with values calculated from the IAPWS [54] formulation. The deviation plot is given in Fig. 1. As one can see from the deviation plot (see Fig. 1), the agreement between IAPWS [54] values and the present results along the isobars (0.1, 10, and 30) MPa is excellent. Deviation statistics for the present viscosity data for

Table III. Experimental Viscosities of Pure Water as a Function of Pressure and Temperature

	η (mPa·s)		
T(K)	0.1 MPa	10 MPa	30 MPa
299.76	0.8591	0.8561	0.8551
315.62	0.6245	0.6234	0.6292
328.37	0.5000	0.5030	0.5071
347.95	0.3761	0.3803	0.3872
375.85	–	0.2772	0.2833
403.95	–	0.2131	0.2181
431.43	–	0.1738	0.1786
476.40	–	0.1326	0.1375
502.75	–	0.1189	0.1239
524.75	–	0.1081	0.1132
549.50	–	0.0961	0.1011
574.54	–	0.0851	0.0918

pure water and values calculated with IAPWS [54] formulation are as follows: AAD = 0.52%, Bias = −0.13%, Std. Dev = 0.61%, Std. Err = 0.13%, and Max Dev = 1.13% ($N = 24$). No systematic trend of the deviations was found for pure water (see Fig. 1). This excellent agreement between the present data and IAPWS [54] values for pure water confirms the reliability of the technique for viscosity measurements on H_2O + K_2SO_4 solutions. This generally good agreement provides confidence in the experimental values of Table IV.

The solutions at the desired compositions were prepared by mass. The composition was checked by comparison of the density of solution at 293.15 K and 0.1 MPa with reference data. Chemically pure K_2SO_4 and distilled water were used to prepare the solutions.

4. RESULTS AND DISCUSSIONS

4.1. Thermal Conductivity

Measurements of the thermal conductivity for the three (0.239, 0.499, and 0.782 mol·kg^{-1}) binary aqueous K_2SO_4 solutions were performed in the temperature range from 298 to 573 K at pressures up to 30 MPa. Measurements were made along three isobars (0.1, 10, and 30 MPa) as a function of temperature for various compositions. The experimental temperature, pressure, composition, and thermal conductivity values are presented in Table II. The values of $T_{aver} = T_1 + 0.5\Delta T$, where T_1 is the temperature of the outer cylinder and ΔT is the temperature difference across the measurement gap, were accepted as experimental temperatures. Some selected experimental results are shown in Figs. 2–5 in the $\lambda - T$, $\lambda - P$, and $\lambda - x$ projections together with values reported by other authors and calculated from various correlation equations from the literature. In Figs. 2a,b and 3 the temperature dependence of the measured values of thermal conductivity for $H_2O + K_2SO_4$ solutions along measured isobars (0.1, 10, and 30 MPa) and selected isopleths are presented. As one can see, each isopleth-isobaric $\lambda - T$ curve go through a maximum, $(\partial\lambda/\partial T)_{PX} = 0$, near 415 K like pure water [37]. For pure water this maximum occurs at temperatures between 409 and 421 K at pressures between 20 and 60 MPa. The pressure and composition dependences of the thermal conductivity maximum for aqueous salt solutions were studied by Abdulagatov and Magomedov [31, 34, 35, 37]. The thermal conductivity maximum of the $H_2O + K_2SO_4$ solutions is shifted to high temperatures as the pressure is increased, while the maximum of the $\lambda - T$ curves decreases with concentration of K_2SO_4.

Table IV. Experimental Viscosities (mPa·s) of $H_2O + K_2SO_4$ Solutions as a Function of Pressure, Temperature, and Concentration

T (K)	0.1 MPa	10 MPa	20 MPa	30 MPa
$m = 0.0658\ mol \cdot kg^{-1}$				
298.15	0.9039	0.9023	0.9040	0.9053
313.55	0.6609	0.6613	0.6650	0.6670
323.25	0.5568	0.5586	0.5601	0.5617
348.45	0.3842	0.3869	0.3912	0.3963
376.65	–	0.2805	0.2846	0.2884
398.55	–	0.2289	0.2321	0.2360
423.85	–	0.1881	0.1926	0.1960
447.35	–	0.1613	0.1645	0.1660
472.05	–	0.1403	0.1436	0.1460
496.35	–	0.1244	0.1276	0.1300
524.45	–	0.1097	0.1135	0.1160
545.05	–	0.1008	0.1045	0.1072
571.55	–	0.0902	0.0940	0.0972
$m = 0.2055\ mol \cdot kg^{-1}$				
298.15	0.9310	0.9297	0.9310	0.9319
311.65	0.7107	0.7122	0.7133	0.7151
323.15	0.5819	0.5837	0.5858	0.5885
348.95	0.3988	0.4020	0.4048	0.4076
365.45	–	0.3303	0.3339	0.3363
396.65	–	0.2435	0.2464	0.2492
425.45	–	0.1946	0.1974	0.2000
448.35	–	0.1679	0.1705	0.1732
477.45	–	0.1430	0.1456	0.1482
497.45	–	0.1294	0.1322	0.1348
523.05	–	0.1162	0.1191	0.1219
550.55	–	0.1039	0.1072	0.1105
574.35	–	0.0940	0.0973	0.1014
$m = 0.3050\ mol \cdot kg^{-1}$				
298.15	0.9616	0.9618	0.9615	0.9640
312.55	0.7172	0.7194	0.7207	0.7227
323.15	0.5972	0.5991	0.6019	0.6045
348.25	0.4147	0.4182	0.4217	0.4248
365.95	–	0.3396	0.3421	0.3460
397.25	–	0.2503	0.2531	0.2565
423.55	–	0.2040	0.2068	0.2096
448.55	–	0.1735	0.1769	0.1790
475.85	–	0.1492	0.1521	0.1545
499.95	–	0.1332	0.1369	0.1400
527.35	–	0.1185	0.1216	0.1243
548.45	–	0.1087	0.1119	0.1150
573.35	–	0.0976	0.1016	0.1035

Table IV. continued

T (K)	0.1 MPa	10 MPa	20 MPa	30 MPa
$m = 0.407\ mol \cdot kg^{-1}$				
298.15	0.9825	0.9823	0.9826	0.9830
312.25	0.7386	0.7414	0.7439	0.7452
323.35	0.6109	0.6130	0.6159	0.6180
348.15	0.4271	0.4316	0.4354	0.4380
372.55	–	0.3265	0.3300	0.3329
396.35	–	0.2605	0.2628	0.2667
422.05	–	0.2131	0.2154	0.2189
446.85	–	0.1811	0.1840	0.1867
470.75	–	0.1586	0.1605	0.1641
498.55	-	0.1388	0.1409	0.1444
523.85	–	0.1248	0.1286	0.1307
541.55	–	0.1171	0.1200	0.1236
575.25	–	0.1021	0.1067	0.1102

Figure 4 shows the results of thermal conductivity measurements for $H_2O + K_2SO_4$ solutions as a function of pressure for selected compositions (4, 8, and 12 mass%) and two selected temperatures (313.15 and 363.15 K). Along each isopleth–isotherm, the thermal conductivity increases almost linearly (the slope $(\partial\lambda/\partial P)_{TX}$ is almost constant) as the pressure increases up to 30 MPa and is not parallel to those of pure water, especially at high K_2SO_4 concentrations and high temperatures (see Fig. 4, see also [31, 51–53]). The slopes of the water isotherms ($\lambda - P$) are slightly higher than the slopes of solution isotherms, especially at high pressures and high K_2SO_4 concentrations.

The composition dependences of the measured thermal conductivities for $H_2O + K_2SO_4$ solutions for selected isotherms–isobars are shown in Fig. 5 together with values calculated with various correlations by other authors. The thermal conductivity of the solution decreases monotonically with composition. As one can see from Fig. 5, the composition dependence of the thermal conductivity is almost linear at concentrations up to 12 mass%, while at high concentrations ($x > 20$ mass%), $\lambda - x$ curves exhibit a small curvature (see, for example, [37]). Extrapolation of the high composition measurements to zero concentration ($x \to 0$) gives values in good agreement with the data for pure water (see Fig. 5) calculated with the IAPWS [54] formulation.

Figures 6 and 7 show direct comparisons of the present thermal conductivity results at atmospheric pressure for $H_2O + K_2SO_4$ solutions with data reported by Vernigora et al. [12] and with values calculated from

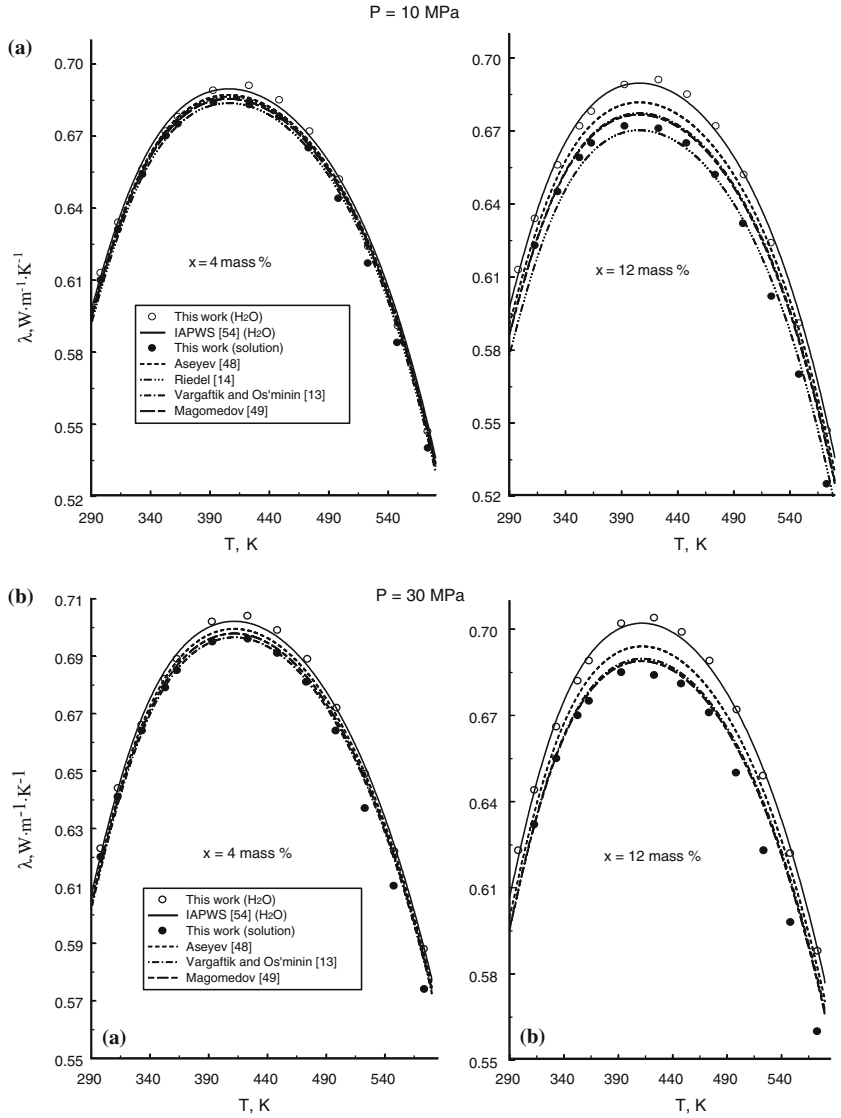

Fig. 2. Measured values of the thermal conductivity of $H_2O + K_2SO_4$ as a function of temperature for isobars at (a) 10 MPa and (b) 30 MPa and at concentrations of 4 and 12 mass% together with data for pure water.

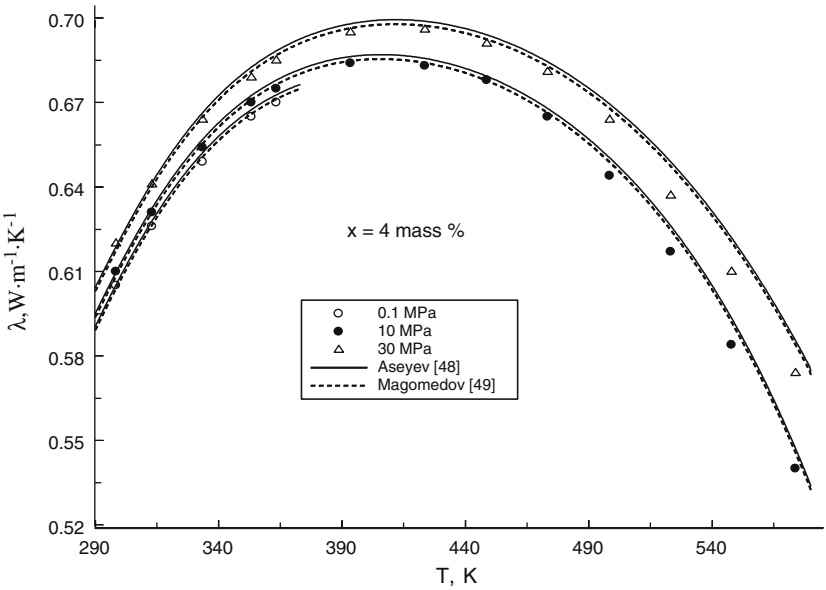

Fig. 3. Measured values of the thermal conductivity of $H_2O + K_2SO_4$ as a function of temperature at a composition of 4 mass% and various pressures (0.1, 10, and 30 MPa) together with values calculated with correlation Eq. (3) by Aseyev [48].

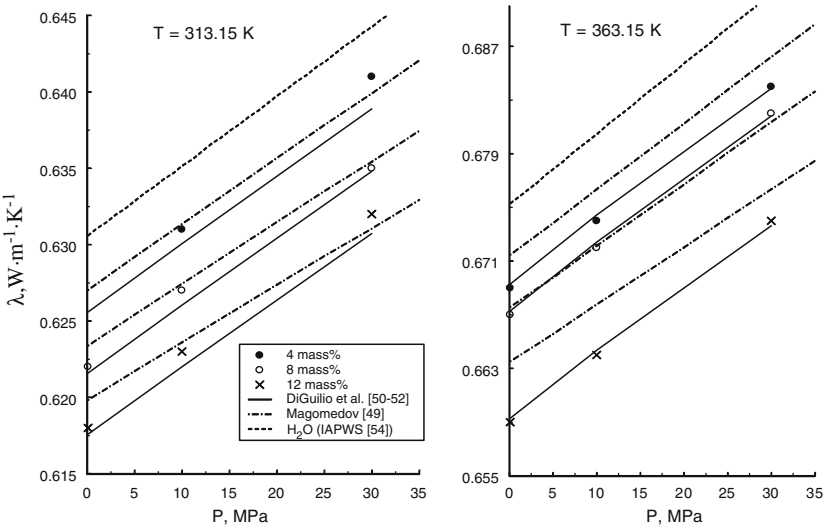

Fig. 4. Measured values of the thermal conductivity of $H_2O + K_2SO_4$ as a function of pressure along isotherms of 313.15 and 363.15 K for various concentrations (4, 8, and 12 mass%) together with values calculated with correlation Eqs. (4) and (5).

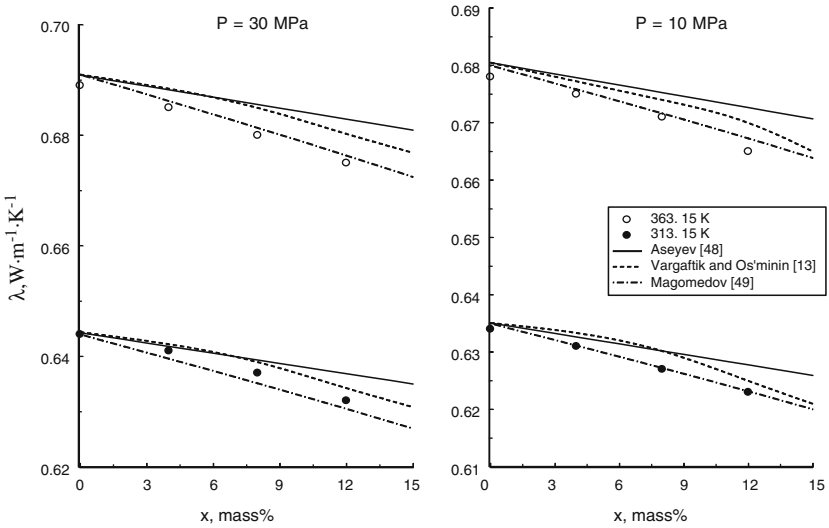

Fig. 5. Measured values of the thermal conductivity of $H_2O + K_2SO_4$ as a function of composition for isobars of 10 and 30 MPa and temperatures of 313.15 and 363.15 K together with values calculated from correlations Eqs. (1), (3), and (4).

correlations (1), (2), and (3) by Vargaftik and Os'minin [13], by Riedel [14], and by Aseyev [48], respectively. The deviation plots for the present data and values calculated with Aseyev [48] (Eq. (3)), DiGuilio [50], DiGuilio and Teja [51], and Bleazard et al. [52, 53] (Eq. (5)) correlations are presented in Figs. 8 and 9. The deviation statistics are given in Table V.

Table V. Deviation Statistics (%) Between Present Thermal Conductivity Results for $H_2O + K_2SO_4$ and Values Calculated with Correlation Eqs. (3) and (4) from Refs. 48 and 49, Respectively

P (MPa)	AAD	Bias	St. Dev	St. Err	Max. Dev
Aseyev [48]					
0.1	0.25	−0.14	0.27	0.07	0.51
10	0.49	−0.23	0.68	0.11	1.98
30	0.48	0.01	0.66	0.11	1.65
All data	0.45	−0.11	0.63	0.07	1.98
Magomedov [49]					
0.1	0.21	−0.11	0.22	0.05	0.46
10	0.27	−0.20	0.51	0.10	1.45
30	0.23	0.005	0.49	0.09	1.02
All data	0.29	−0.10	0.38	0.06	1.45

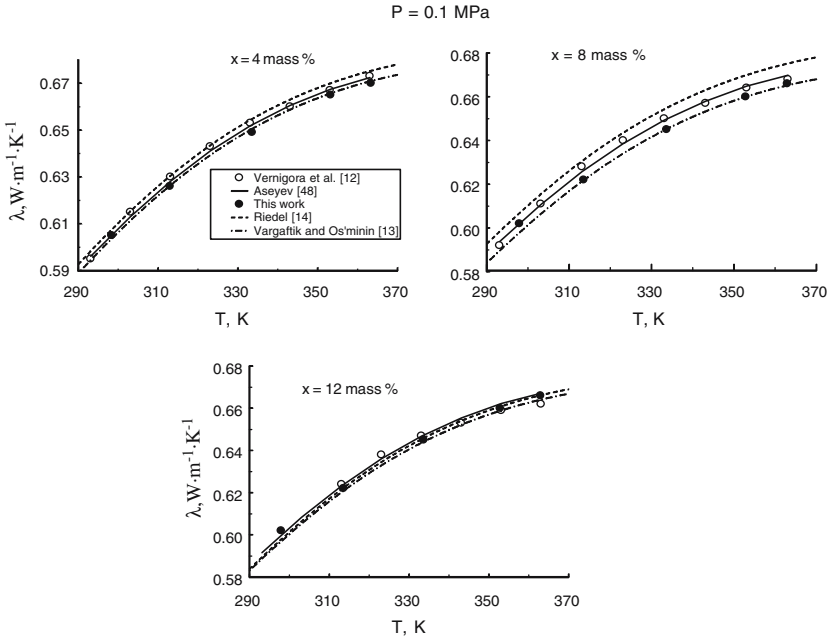

Fig. 6. Comparisons of the present experimental thermal conductivity data for $H_2O + K_2SO_4$ solutions with data reported by Vernigora et al. [12] and values calculated from correlation Eqs. (1) to (3) at atmospheric pressure for various compositions.

As one can see from Figs. 8 and 9 and Table V, the agreement between the present and literature results is good (deviations within ±0.5%). Excellent agreement within 0.2% between measured and calculated values with DiGuilio [50], DiGuilio and Teja [51], and Bleazard et al. [52, 53] correlation (5) is found at all concentrations and temperatures up to 363.15 K and at pressures up to 30 MPa. Initially the correlation (Eq. (3)) by Aseyev [48] was developed for temperatures up to 373.15 K and at a pressure of 0.1 MPa. As Figs. 2a, b to 8 show, this correlation shows excellent agreement with the data at high pressures and high temperatures. Excellent agreement (within 0.2% at high temperatures and 0.6% at low temperatures) is found between the present data and values reported by Vernigora et al. [12] (see Figs. 6 and 7). Figures 6 and 7 demonstrate that the data reported by Vernigora et al. [12] for $H_2O + K_2SO_4$ solutions at concentrations of (4 and 8) mass% are systematically higher (by 0.5–0.8%) than the present data, while at a concentration of 12 mass%, no systematic deviations larger than 0.2% are found.

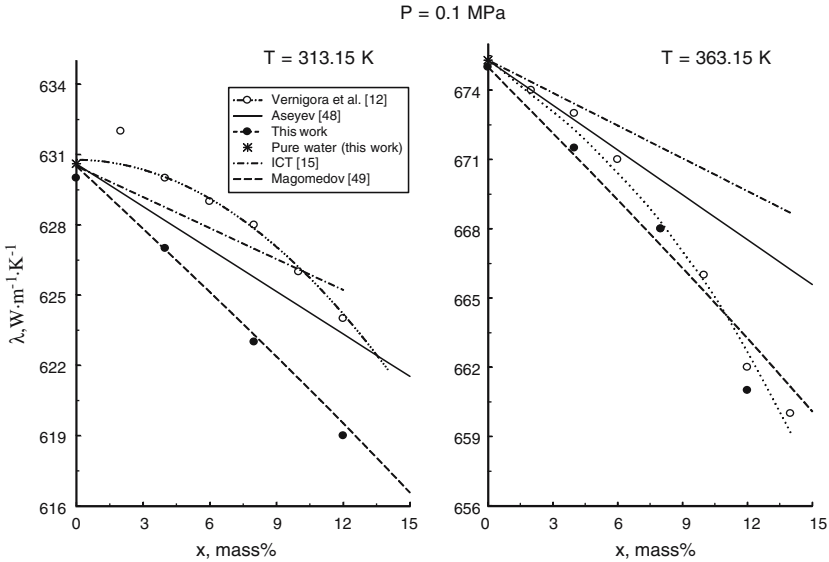

Fig. 7. Comparisons of concentration dependence of the present experimental thermal conductivity results for $H_2O + K_2SO_4$ solutions with data reported by Vernigora et al. [12] and values calculated from correlation Eqs. (3) and (4) at atmospheric pressure for temperatures of 313.15 and 363.15 K.

Figure 10 shows the concentration dependence of the thermal conductivity of a series of aqueous solutions with the same anion (negative ion SO_4^{-2}) and various cations (positive ions K^+, Na^+, Li^+, Mg^{2+}, Zn^{2+}, and Cu^{2+}). This figure demonstrates the effect of various cations on the values and behavior of the thermal conductivity of salt solutions (sulfates). As one can see from Fig. 10, the $H_2O + K_2SO_4$ solution shows intermediate values of thermal conductivity among other aqueous (Na_2SO_4, Li_2SO_4, $MgSO_4$, $ZnSO_4$, and $CuSO_4$) solutions at the same thermodynamic (P, T, x) conditions, while the thermal conductivity of $H_2O + Li_2SO_4$ and $H_2O + Na_2SO_4$ solutions show highest and lowest values, respectively.

4.2. Viscosity

The viscosity measurements for four (0.0658, 0.2055, 0.3050, and 0.4070 mol·kg^{-1}) binary aqueous K_2SO_4 solutions have been made at temperatures from 298 to 573 K at pressures up to 30 MPa. All experimental viscosity data were obtained as a function of temperature for four

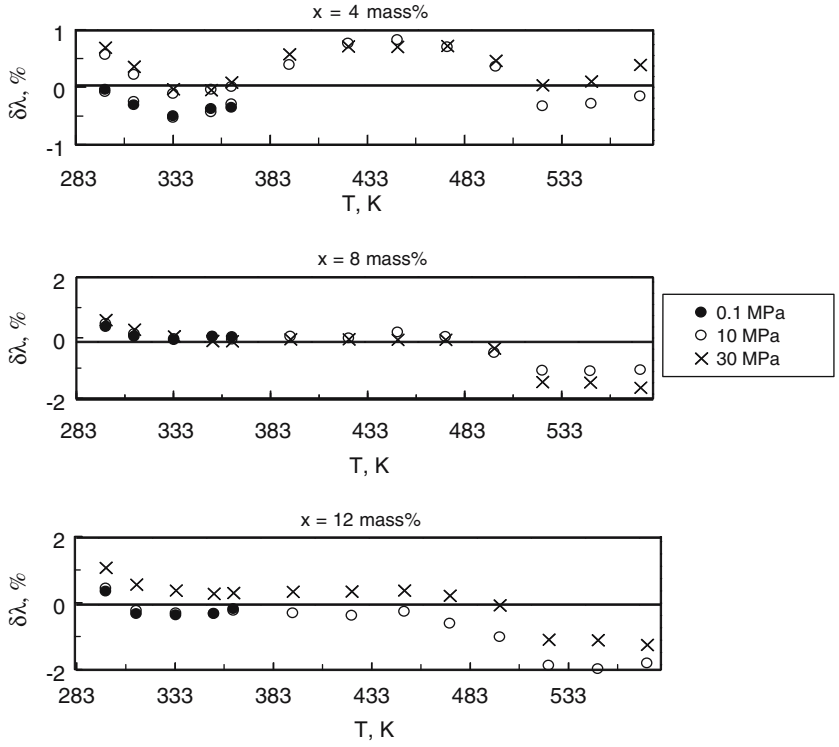

Fig. 8. Thermal conductivity deviations, $\delta\lambda = 100(\lambda_{exp} - \lambda_{cal})/\lambda_{exp}$, of experimental results for $H_2O + K_2SO_4$ solutions from values calculated with correlation Eq. (3) by Aseyev [48] as a function of temperature at selected concentrations.

isobars (0.1, 10, 20, and 30 MPa). The experimental temperature, viscosity, pressure, and composition values for the aqueous K_2SO_4 solutions are presented in Table IV. Some selected experimental viscosity data for $H_2O + K_2SO_4$ solutions, as examples of the present results, are shown in Figs. 11–14 in the $\eta - T$, $\eta - P$, and $\eta - m$ projections together with values calculated from the IAPWS [54] formulation for pure water ($m = 0$). Figures 11 to 14 also contain data reported by other authors and calculated with correlation Eqs. (6) and (7) by Correia and Kestin [17] and Zaytsev and Aseyev [16], respectively. Figures 11 and 12 shows the temperature dependence of the experimental values of the viscosity for $H_2O + K_2SO_4$ solutions, 0.2055 and 0.3050 mol·kg^{-1}, at fixed pressures of 0.1 and 10 MPa together with values reported by other authors. In the temperature range from 298 to 385 K, the viscosity of the solution decreases sharply (factor of six) with temperature. As one

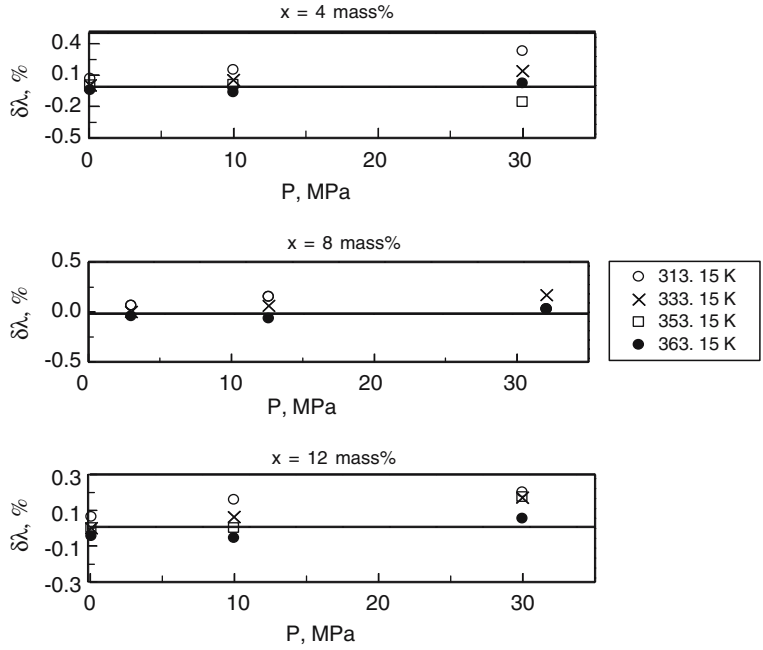

Fig. 9. Thermal conductivity deviations, $\delta\lambda = 100(\lambda_{exp} - \lambda_{cal})/\lambda_{exp}$, of experimental results for $H_2O + K_2SO_4$ solutions from values calculated with correlation Eq. (5) by DiGuilio et al. [50], DiGuilio and Teja [51], and Bleazard et al. [52, 53] as a function of pressure for selected isotherms.

can see from Fig. 13, the viscosity of the solution at constant composition ($m = 0.3050\,\text{mol}\cdot\text{kg}^{-1}$) and selected temperatures slightly increases linearly as the pressure increases (the slopes $(\partial\eta/\partial P)_{TX}$ of the $\eta - P$ curves are almost constant). The viscosity is little affected (up to 8%) at high temperatures (573 K) and (up to 0.1%) at low temperatures (298 K) by pressure (pressure change between 0.1 and 30 MPa) along the isotherms (see Fig. 13). As Fig. 14 shows, the viscosity of $H_2O + K_2SO_4$ solutions increases monotonically with concentration at constant pressure and temperature (isobars–isotherms).

The present experimental values for the viscosity of $H_2O + K_2SO_4$ solutions were directly compared with data reported by other authors in the literature. Figures 11, 12, and 14–16 show the values of viscosity reported by various authors from the literature together with the present results. These figures include also the values of viscosity for $H_2O + K_2SO_4$ solutions calculated with correlation Eqs. (6) and (7) reported by Correia and Kestin [17] and Zaytsev and Aseyev [16], respectively. As one can

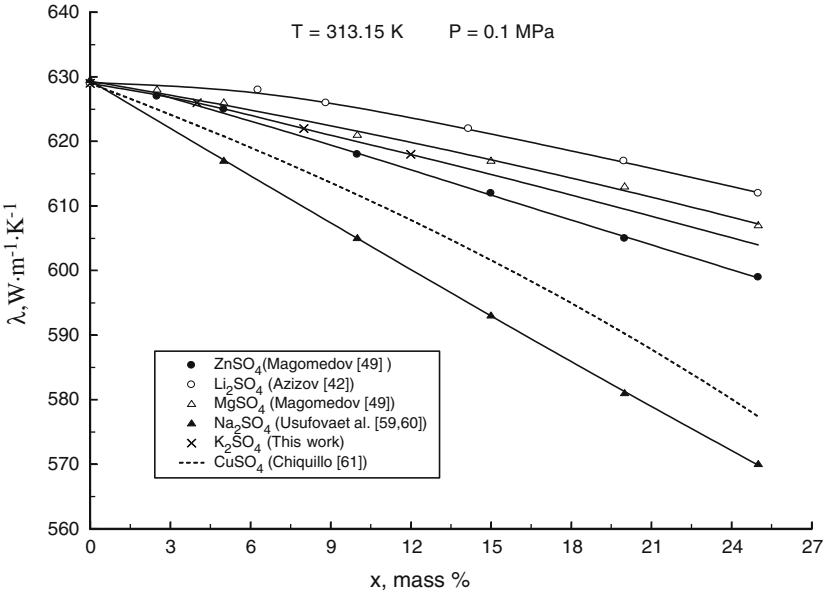

Fig. 10. Thermal conductivity of a series of aqueous solutions as a function of composition at 313.15 K and 0.1 MPa reported by various authors.

see from these figures, the agreement between various data sets is good. Figures 11, 12, and 14–16 illustrate that our data are consistent with literature values at atmospheric and high pressures and various temperatures. Excellent agreement within ±0.85% is observed between present measurements and data reported by Maksimova et al. [19] at atmospheric pressure and at temperatures up to 363 K. Excellent agreement within ±0.54% was also found between the present results and data reported by Puchkov and Sargaev [18]. The data reported by Kaminsky [21] show deviations within 1.0%. Good agreement within 0.06–1.19% was found with the data reported by Jones and Colvin [22] at a temperature of 298.15 K and atmospheric pressure. The data reported by Tanaka [25] differ from the present results by 0.28–1.44%. Good agreement (AAD = 0.56%) is found also between the data reported by Sulston [27] and the present data. Differences between our measurements and values calculated with correlation Eq. (6) are within 0.5–1.0%, which is less than the experimental uncertainty. Deviation plots between the present data and values calculated with correlation Eqs. (6) and (7), at atmospheric pressure and high pressures, are given in Figs. 17 and 18. Table VI shows the deviation statistics for the correlations, Eqs. (6) and (7), for the various isobars and all

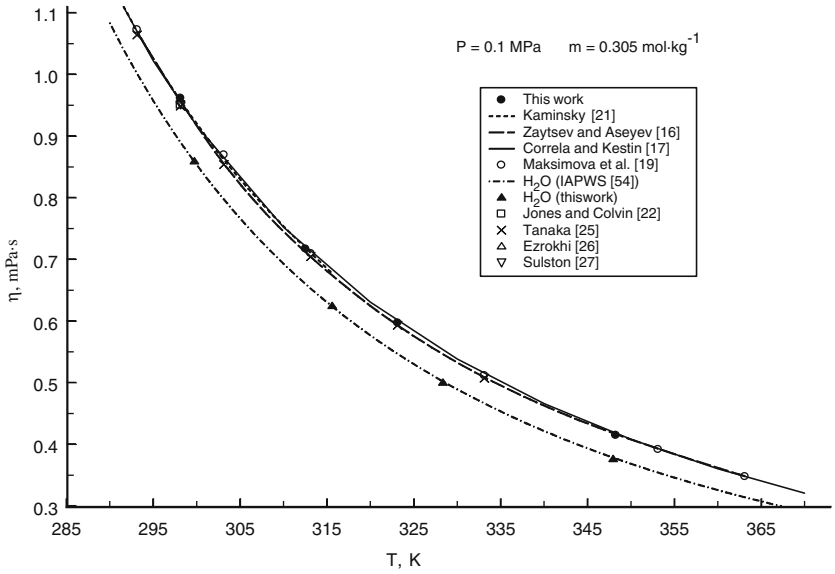

Fig. 11. Measured values of the viscosity of $H_2O + K_2SO_4$ solutions as a function of temperature at a concentration of 0.3050 mol·kg^{-1} and at atmospheric pressure together with values reported by other authors in the literature.

Table VI. Deviation Statistics (%) Between Present Viscosity Results for $H_2O + K_2SO_4$ and Values Calculated with Correlation Eqs. (6) and (7) from Refs. 17 and 16, Respectively

P (MPa)	AAD	Bias	St. Dev	St. Err	Max. Dev
Correla and Kestin [17]					
0.1	0.46	0.22	0.50	0.12	0.95
10	0.59	−0.26	0.68	0.15	1.50
20	0.86	−0.46	0.95	0.21	2.00
30	0.93	−0.84	0.92	0.24	2.80
All data	0.78	−0.49	0.87	0.12	2.80
Zaytsev and Aseyev [16]					
0.1	0.41	0.36	0.40	0.10	1.0
10	0.70	−0.40	0.78	0.14	1.78
20	0.77	0.52	0.74	0.19	1.76
30	0.87	0.47	0.87	0.22	1.51
All data	0.76	0.04	0.90	0.12	1.78

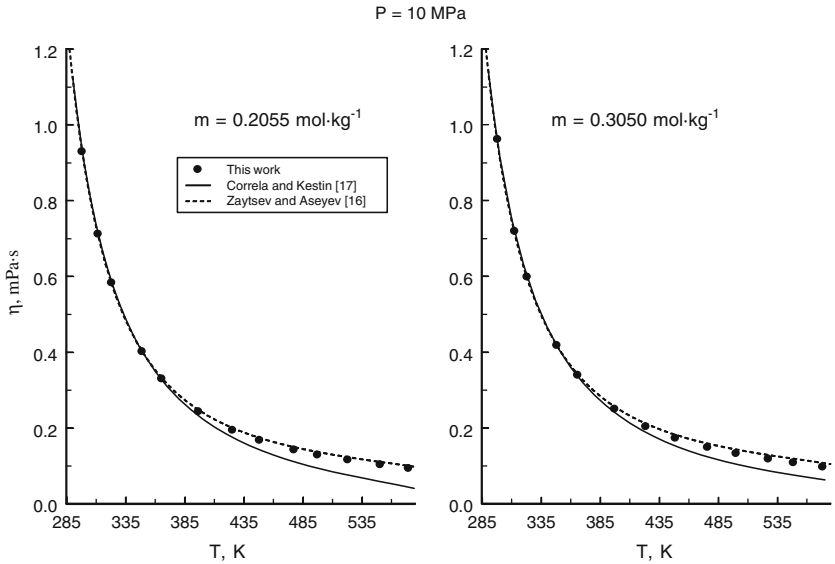

Fig. 12. Measured values of the viscosity of $H_2O + K_2SO_4$ solutions as a function of temperature at selected concentrations (0.2055 and 0.3050 mol·kg^{-1}) and at 10 MPa together with values calculated with correlation Eqs. (6) and (7).

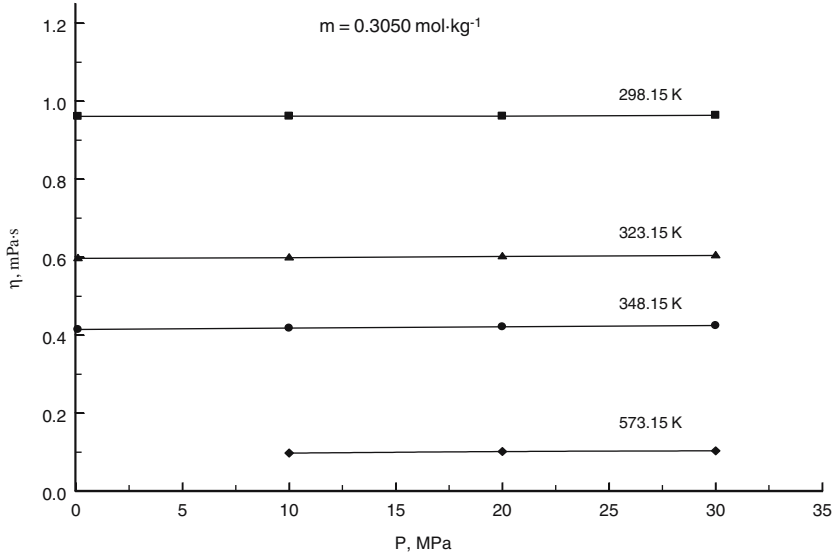

Fig. 13. Measured values of the viscosity of $H_2O + K_2SO_4$ solutions as a function of pressure at a concentration of 0.3050 mol·kg^{-1} and at various temperatures.

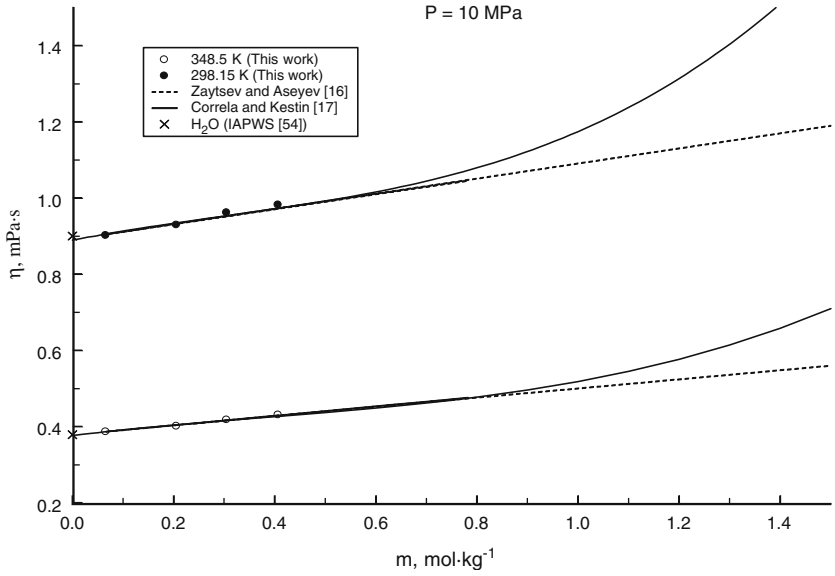

Fig. 14. Measured values of the viscosity of $H_2O + K_2SO_4$ solutions as a function of concentration m along isotherms at 298.15 and 348.50 K and at a pressure of 10 MPa together with values calculated with correlation Eqs. (6) and (7).

of the data. The correlation (Eq. (6)) is valid at temperatures from 293 to 363 K and at pressures up to 30 MPa. As Fig. 12 shows, extrapolation of the calculations with Eq. (6) to high temperatures (up to 495 K) still gives values in reasonable (within 3%) agreement with present experimental data. Although Eq. (7) was initially developed by Zaytsev and Aseyev [16] for atmospheric pressure and for temperatures up to 373 K, one can see from Fig. 12 that this equation yield the correct temperature dependence of the viscosity data at high pressures, while the concentration dependence of this equation at $m > 0.6\,\text{mol}\cdot\text{kg}^{-1}$ is incorrect.

Figure 19 shows the concentration dependence of the viscosity of a series of aqueous solutions with the same anion (negative ion SO_4^{-2}) and various cations (positive ions K^+, Na^+, Li^+, Mg^{2+}, and Ni^{2+}). This figure demonstrates the effect of various cations on the values and behavior of the viscosity of salt solutions (sulfates). As one can see from Fig. 19 the $H_2O + K_2SO_4$ solution showed smallest values of the viscosity compared to other aqueous (Na_2SO_4, Li_2SO_4, $MgSO_4$, and Ni_2SO_4) solutions at the same thermodynamic (P, T, x) conditions, while the viscosity of $H_2O + Ni_2SO_4$ solution showed highest values.

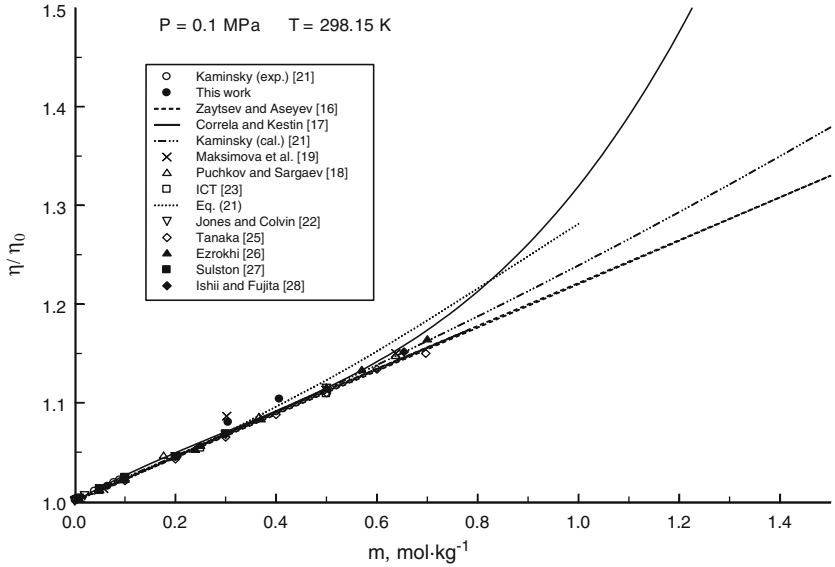

Fig. 15. Measured values of the relative viscosity (η/η_0) of $H_2O + K_2SO_4$ solutions as a function of concentration m along an isotherm of 298.15 K and at atmospheric pressure together with values reported by other authors and calculated with correlation Eqs. (6) and (7).

The measured viscosities for $H_2O + K_2SO_4$ solutions were used to calculate the viscosity A-, B-, and D-coefficients of the extended Jones–Dole equation for various isotherms. The values of the viscosity A- and B-coefficients of an electrolyte provide information on the interaction between dissolved ions (K^+, SO_4^{2-}) and molecules of a solvent (H_2O). For example, the A-coefficient of the Jones–Dole equation is determined by ion-atmosphere interactions and ionic mobilities and can be calculated from theory [62, 63]. Low concentration viscosity measurements for most aqueous electrolyte solutions show good agreement between experiment and theory [21, 64–67]. The second Jones–Dole parameter B is related to the size and shape of the ions and the solute-solvent interactions [4]. Therefore, the viscosity A- and B-coefficients of electrolyte solutions are useful tools to study structural interactions (ion-ion, ion-solvent, and solvent-solvent) in solutions. An extensive compilation of Jones–Dole A- and B-coefficients for a series of aqueous electrolyte solutions is reported by various authors [4, 5, 21, 64–77].

The viscosity B-coefficient for aqueous solutions shows a strong temperature dependence, which can be attributed to ion-solvent interactions. However, measurements of the temperature dependence of the A- and

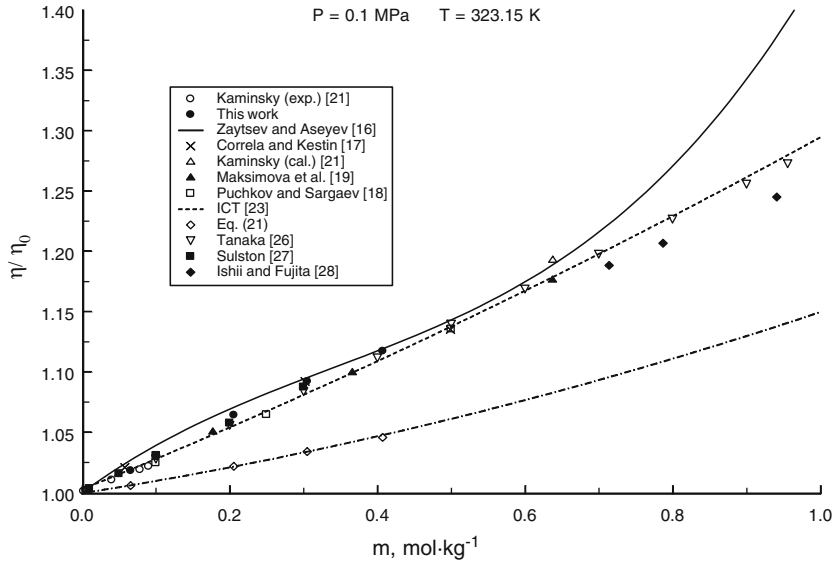

Fig. 16. Measured values of the relative viscosity (η/η_0) of $H_2O + K_2SO_4$ solutions as a function of concentration m along an isotherm of 323.15 K and at atmospheric pressure together with values reported by other authors and calculated with correlation Eqs. (6) and (7).

B-coefficients have so far been limited to rather narrow ranges of temperature (up to 368 K) with less satisfactory accuracy. We examine the viscosity A- and B-coefficients values of aqueous K_2SO_4 solutions as a function of temperature in the temperature range from 298 to 373 K. We have also extended the concentration range of the viscosity measurements to accurately determine a higher-order coefficient (viscosity D-coefficient) for the extended Jones–Dole equation.

Falkenhagen–Onsager–Fuoss [78, 79] and Debye–Hückel–Onsager [80, 81] theories predict a square-root concentration, $\eta/\eta_0 \propto \sqrt{c}$, dependence of the viscosity of ionic solutions at infinite dilution ($x \to 0$). This theory correctly explains the rise of viscosity with concentration in the limit of very low (dilute solutions) ion concentrations ($c < 0.05\,\mathrm{mol\cdot L^{-1}}$). This model was based on macroscopic considerations. Therefore, this model is inadequate when intermolecular correlations become important. Jones and Dole [82] proposed an empirical extension of the Falkenhagen [62] model to high concentrations as

$$\frac{\eta}{\eta_0} = 1 + A\sqrt{c} + Bc, \tag{14}$$

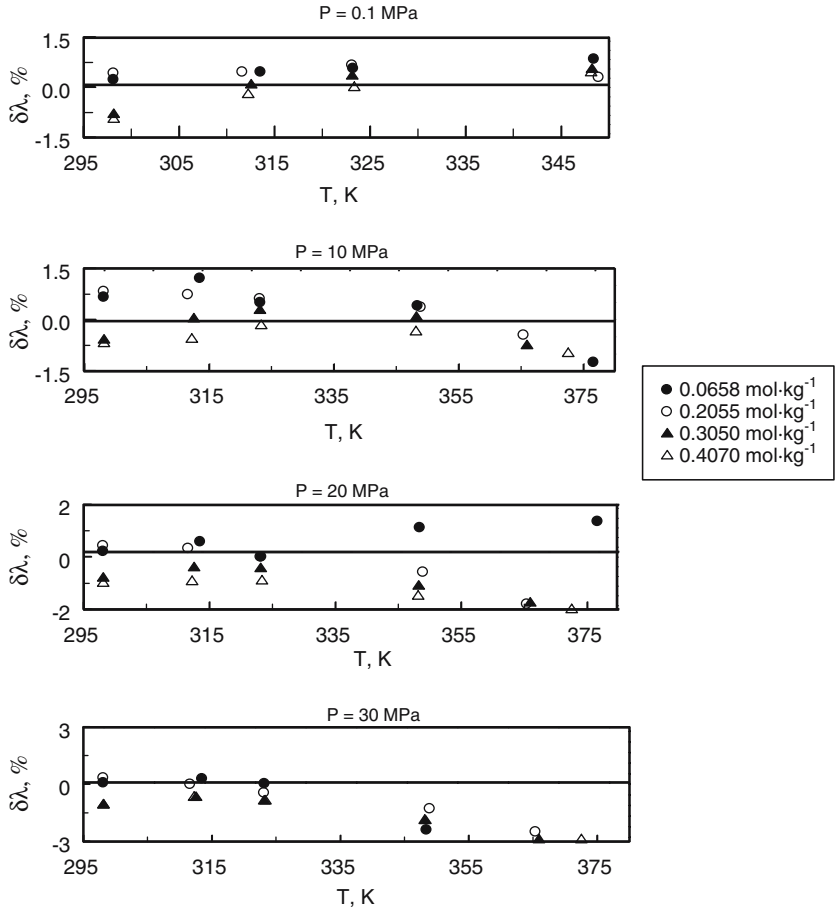

Fig. 17. Viscosity deviations, $\delta\eta = 100(\eta_{exp} - \eta_{cal})/\eta_{exp}$, of the experimental results for $H_2O + K_2SO_4$ from values calculated with correlation Eq. (6) by Correia and Kestin [17] as a function of temperature for various compositions.

for the viscosity of electrolyte solutions. In Eq. (14) η and η_0 are the viscosities of an electrolyte solution and pure solvent (water), respectively, A is an always positive constant, and c is the electrolyte molarity concentration (in mol·L^{-1}). The viscosity A-coefficient is related to the long-range Coulombic force interactions and the mobilities of solute ions, and B is related to the interactions between the solvent and ions and the ion size. The sign of the B-coefficient depends on the degree of solvent structuring introduced by the ions. A positive value of the B-coefficient is associ-

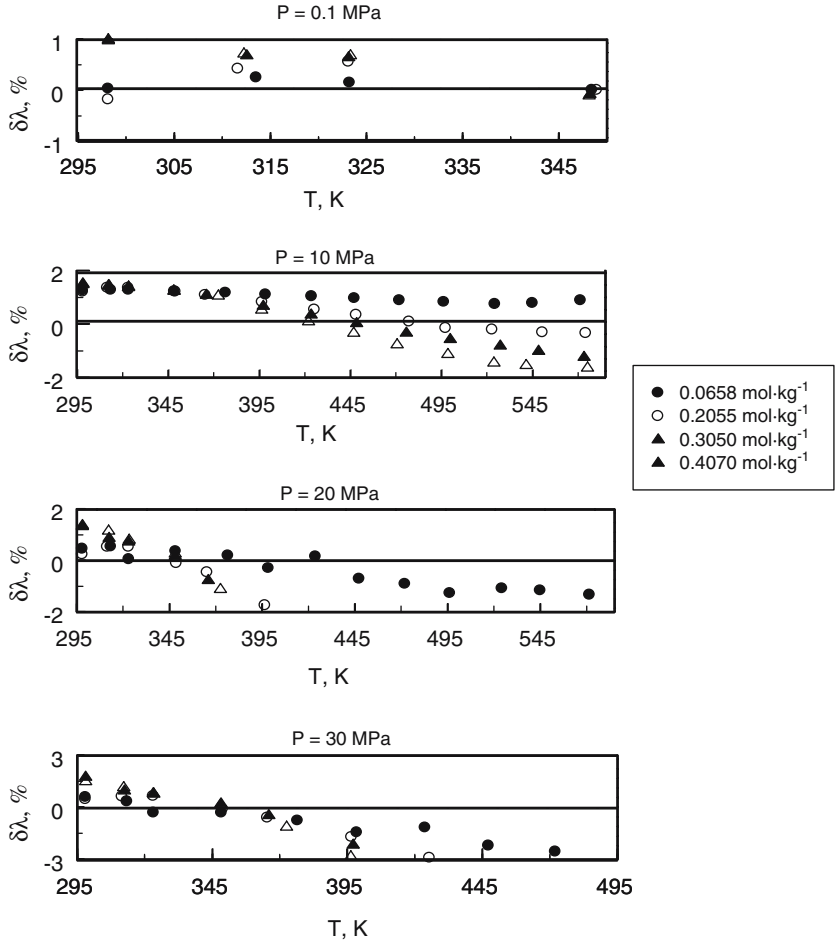

Fig. 18. Viscosity deviations, $\delta\eta = 100(\eta_{exp} - \eta_{cal})/\eta_{exp}$, of the experimental results for $H_2O + K_2SO_4$ from values calculated with correlation Eq. (7) by Zaytsev and Aseyev [16] as a function of temperature for various compositions.

ated with structure-making (ordering) ions, while a negative value of the *B*-coefficient is associated with structure-breaking (disordering) ions. This equation is valid only for concentrations below 0.1 mol·L^{-1}, although theory cannot exactly predict the concentration range where Eq. (14) is valid. The values of the parameters in Eq. (14) were determined over various fitted concentration ranges. The optimal concentration range also depends on temperature. Equation (14) provides a better description of the exper-

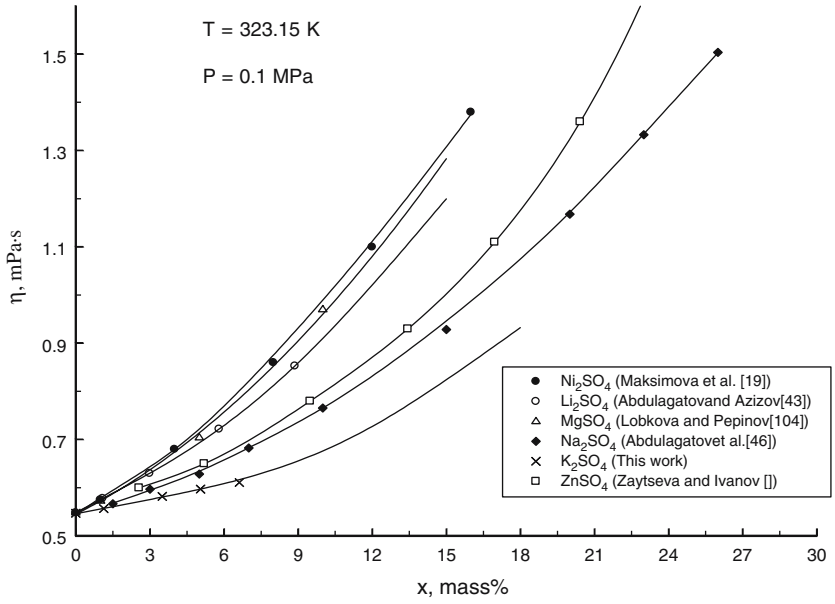

Fig. 19. Viscosity of a series of aqueous solutions as a function of composition at 323.15 K and 0.1 MPa reported by various authors.

imental viscosity data than $\eta/\eta_0 = 1 + A\sqrt{c}$. Falkenhagen and Dole [79] gave a theoretical derivation of the A-coefficient. Its general form is

$$A = \frac{A^*}{\eta_0(\varepsilon_0 T)^{1/2}} f(\lambda_+^\infty, \lambda_-^\infty, z_+, z_-), \tag{15}$$

where

$$A^* = \frac{Fe^2 N_A^{1/2}(1+\sqrt{2})}{12\pi(\varepsilon^* k)^{1/2}} \text{ and}$$

$$f = \frac{z^2\left(\lambda_+^\infty + \lambda_-^\infty\right)}{4\left(2+\sqrt{2}\right)\left(\lambda_+^\infty \lambda_-^\infty\right)}\left[1 - \frac{4\left(\lambda_+^\infty - \lambda_-^\infty\right)^2}{\left(1+\sqrt{2}\right)^2\left(\lambda_+^\infty + \lambda_-^\infty\right)^2}\right]. \tag{16}$$

where $A^* = 1.113 \times 10^{-5\circ}\text{C}^2(\text{m}\cdot\text{K}\cdot\text{mol}^{-3})^{1/2}$, $f(\lambda_+^\infty, \lambda_-^\infty, z_+, z_-)$ is a function of the equivalent conductances $\lambda_\pm^\infty$ at infinite dilution of the ions, and $z_\pm$ represents the charges. The value of parameter A depends also on the viscosity of the solvent η_0, its relative permittivity (dielectric constant) ε_0, and the temperature T.

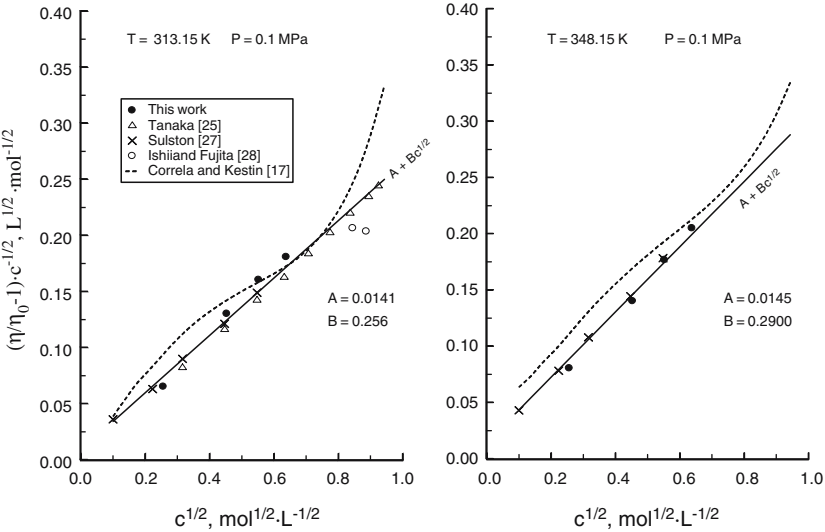

Fig. 20. Jones–Dole plot, $[(\eta/\eta_0)-1]/c^{1/2}$ vs. $c^{1/2}$ for $H_2O + K_2SO_4$ solutions for iso therms of 313.15 and 348.15 K at atmospheric pressure.

Present experimental data for the relative viscosity η/η_0 at various temperatures, together with data reported by other authors at low concentrations [21–28], were used to calculate A- and B-coefficients in the Jones and Dole [82] Eq. (14). According to a conventional technique of determining the viscosity coefficient, the B- and D-coefficients can be estimated from experimental viscosity data by extrapolating the function,

$$B + Dc = \frac{(\eta/\eta_0) - 1 - Ac^{1/2}}{c}, \tag{17}$$

to zero concentration, using the theoretical value of A or the slope of the $[(\eta/\eta_0)-1]/c^{1/2}$ vs. $c^{1/2}$ dependence (Jones–Dole plot, see Fig. 20);

$$[(\eta/\eta_0)-1]/c^{1/2} = A + Bc^{1/2}. \tag{18}$$

The present viscosity data for $H_2O + K_2SO_4$ solutions, together with data reported by other authors, are presented in Fig. 20 in a Jones–Dole plot, $[(\eta/\eta_0)-1]/c^{1/2}$ versus $c^{1/2}$ for the selected temperatures (313.15 and 348.15 K). The coefficients A and B, the intercept and slope of a Jones–Dole plot, respectively, were calculated using least-squares analysis of the present data and the data reported in other studies from the literature for various temperatures. As Fig. 20 shows, the data lie on a straight

Table VII. Viscosity A-, B-, and D-Coefficients of Aqueous K_2SO_4 Solutions as a Function of Temperature

T (K)	A ($dm^{3/2}\cdot mol^{-1/2}$)	B ($dm^3\cdot mol^{-1}$)	D ($dm^6\cdot mol^{-2}$)
$P = 0.1$ MPa			
298.15	0.0136	0.195	0.0330
313.15	0.0140	0.256	0.0197
323.15	0.0145	0.280	0.0141
348.15	0.0145	0.310	0.0023
$P = 10$ MPa			
298.15	0.0113	0.2150	0.0630
323.15	0.0112	0.2800	0.0600
348.15	0.0144	0.2960	0.0644
373.15	0.0138	0.3021	0.1084
423.15	0.0144	0.3178	0.1286
473.15	0.0145	0.3500	0.1400
523.15	0.0148	0.4091	0.1739
573.15	0.0405	0.4525	0.3235

line with negligible scatter in the concentration range $c < 0.3\,mol\cdot L^{-1}$, but this concentration range perhaps changes with temperature. The results are summarized in Table VII and presented in Fig. 21a, b as a function of temperature together with values reported by other authors and calculated from theory. As one can see from Fig. 21a, b the agreement between A- and B-coefficients derived in the present study and those calculated with theory and ionic B-coefficient data is good. Figure 21a, b demonstrates that both A- and B-coefficients go through a maximum ($dB/dT = 0$) near 335 K. At temperatures below about 335–340 K, the derivative (temperature coefficient) $dB/dT > 0$ (structure-breaking ions) is positive, while above the temperature of 323 K, $dB/dT < 0$ (structure-making ions) [69, 83, 84].

The B-coefficients, obtained by other authors for other aqueous electrolyte solutions in all previous studies (except Millero et al. [85]), increase almost linearly (see Fig. 21b) with temperature in the temperature range up to 313 K. Kaminsky [84] and Millero et al. [85] showed that the B-coefficient goes through a maximum near 318–323 K for some electrolyte solutions (for example, for $H_2O + Na_2SO_4$). Since the B-coefficient is proportional to the partial molar volume of a salt $\bar{V}$ ($B = k\bar{V}$; see, for example, Refs. 69, 72, and 76), or hydration volume, one would expect (dB/dT) to be proportional to ($d\bar{V}/dT$). As has been shown by various authors (see, for example, Refs. 86–94) for aqueous electrolyte solutions, the partial molar volume $\bar{V}$ also goes through a maximum within the same temperature range. Our

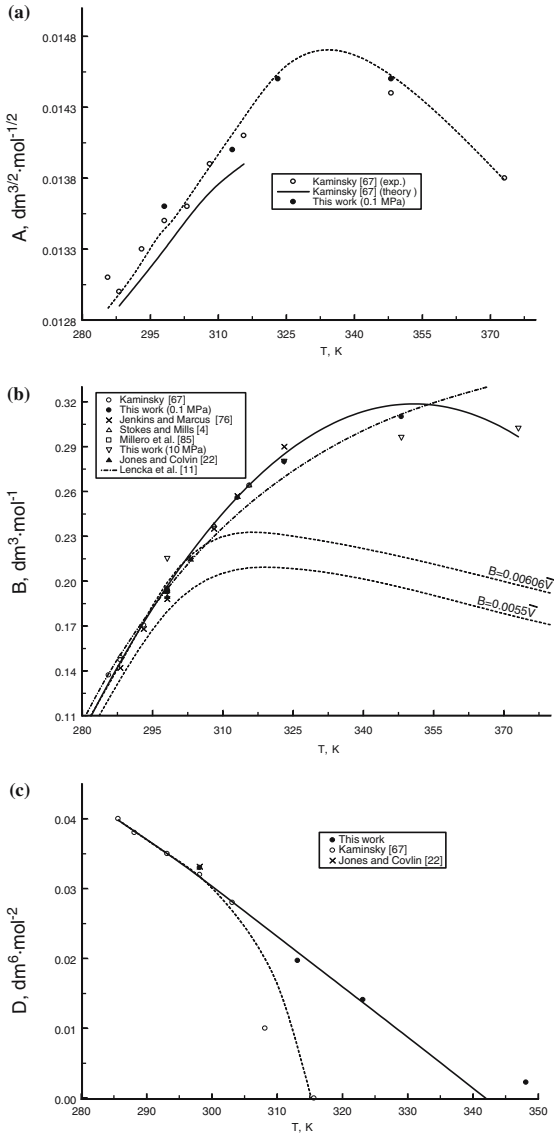

Fig. 21. Experimental viscosity (a) *A*-, (b) *B*-, and (c) *D*-coefficients of $H_2O + K_2SO_4$ solutions as a function of temperature together with values reported by other authors from the literature. Dashed curve is a guide for the eye.

earlier $PVTx$ and partial molar volume measurements [58] for K_2SO_4 (aq) showed that the partial molar volume goes through a maximum at a temperature of about 323 K. Therefore, indirect studies of the volumetric properties of K_2SO_4 (aq) confirmed the presence of a maximum in the temperature dependence of the B-coefficient.

Einstein [95] has calculated the size effect (hydrodynamic effect) for an infinitely dilute suspension of rigid spherical particles in a continuum and obtained the following expression:

$$\frac{\eta}{\eta_0} = 1 + k\phi, \tag{19}$$

where ϕ is the volume fraction of the solute molecules ($\phi = \frac{4}{3}\pi R^3 N_A c$, where R is the effective solute ion radius). For solid spheres with a diameter large compared to molecular dimensions, the value of k in Eq. (19) is commonly accepted to be 2.5, although values as large as 5.5 have been suggested by Happel [96]. If ϕ is expressed in terms of the concentration (in $\text{mol}\cdot\text{L}^{-1}$), then Eq. (19) becomes [63, 72]

$$\frac{\eta}{\eta_0} = 1 + 2.5 V_k c, \tag{20}$$

where V_k is the hydrodynamic molar volume in $\text{cm}^3\cdot\text{mol}^{-1}$. If Einstein's Equation (20) is related to the Jones–Dole Equation (14), the B-coefficient can then be related to the molar volume V_k by $B = 2.5V_k$. As discussed by Desnoyers and Perron [72], V_k should be given by the partial molar volume of the solute $\bar{V}$, although other authors (for example, Skinner and Fuoss [97]) considered V_k as the apparent molar volume. Thomas [98] has extended the Einstein relation Eq. (20) for the hydrodynamic effect to high concentrations by showing that for suspensions the relative viscosity is given by the relation,

$$\frac{\eta}{\eta_0} = 1 + 2.5\phi + 10.05\phi^2 = 1 + 2.5V_k c + 10.05V_k^2 c^2. \tag{21}$$

As was shown by Breslau and Miller [99], this relation can be used to represent the concentration dependence of the relative viscosity for concentrated electrolyte solutions if V_k is taken as an adjustable parameter. They determined the value of $V_k = 0.0324\,\text{L}\cdot\text{mol}^{-1}$ for $H_2O + K_2SO_4$ in Eq. (21) in the concentration range from 0.125 to $1.0\,\text{mol}\cdot\text{L}^{-1}$. Moulik and Rakshit [100] also used Eq. (21) to correlate the concentration dependence of the viscosity of electrolyte solutions at high concentrations. We used experimental partial molar volumes for $H_2O + K_2SO_4$ solutions [58] to calculated relative viscosity values with Eq. (21). The results are shown

in Fig. 16. As Fig. 16 shows, calculated values of the relative viscosity are sufficiently lower than experimental values (the difference $B - 2.5\bar{V}$ is positive, therefore, according to Desnoyers and Perron [72], $H_2O + K_2SO_4$ solutions are structure makers). This means that the theoretical values of the coefficients (0.25 and 10.05) in Eq. (21) are not correctly taking into account the shape and size effects on the flow pattern or the values of the hydrostatic volume (effective volume fraction of the solute molecules) are sufficiently larger than the partial molar volume ($V_k \gg \bar{V}$). Equation (21) can be used to estimate the values of the hydrostatic volume by using experimental relative viscosity data.

Cox and Wolfenden [77] assumed the additivity of the ionic B-coefficients. This additivity, $B = \sum \nu_i B_i$, where the summation extends over all the ions present and the ionic B-coefficients B_i. The values of B_i are constant at a given T for given ions in a specific solvent and describe solely the ion-solvent interactions. The present results for the B-coefficient show satisfactory agreement with the data estimated from the additivity principle (see Fig. 21b).

The viscosity B-coefficient for K_2SO_4(aq) is positive (see Fig. 21b). Typically, large positive values of the B-coefficient are found for ions that are strongly hydrated. At 298.15 K the B-coefficients value for K^+ is -0.009 (slightly structure-disordering ion) and 0.206 for SO_4^{-2} (structure-ordering ion). The values of the B-coefficients for K^+ and SO_4^{-2} become more positive as the temperature increases [76]. There are other types of electrolyte solutions (for example, $H_2O + KNO_3$, $H_2O + KBr$, $H_2O + KCl$, $H_2O + KI$, $H_2O + RbCl$, and $H_2O + CsCl$) for which the viscosity decreases with concentration at low electrolyte concentrations, reaches a minimum value, and then increases monotonically for higher concentrations. For these type electrolyte solutions, the B-coefficient is negative. The experimentally observed viscosity changes result from competition between various effects occurring in the ionic neighborhood. At a given concentration the B-coefficient can be interpreted in terms of a competition between specialized viscosity effects such as coulombic interactions, size and shape of effects or the Einstein effect, alignment or orientation of polar molecules by the ionic field, and distortion of the solvent structure [4]). These effects are governing the viscosity behavior of the aqueous electrolyte solutions.

Jones and Talley [65], Kaminsky [21, 67], Desnoyers and Perron [72], Feakins and Lawrence [101], Desnoyers et al. [102], and Robertson and Tyrrell [103], added a quadratic term (extended Jones–Dole equation),

$$\frac{\eta}{\eta_0} = 1 + A\sqrt{c} + Bc + Dc^2, \tag{22}$$

to extend the Jones–Dole equation to more concentrated electrolyte solutions ($c < 0.1$ to 0.2 m). The new Dc^2 term of Eq. (22) includes all solute–solvent and solute–solute structural interactions that were not accounted by the $A\sqrt{c}$ and Bc terms at high concentrations such as [4, 72]: higher-order terms of the long-range coulombic forces; higher-order term hydrodynamic effect; and interactions arising from changes in solute–solvent interactions with concentration. The range of the concentration in the present study overlaps the range where the Bc term is essential. In the present study we used Eq. (22) for application at higher concentrations. The relative viscosities for K_2SO_4 (aq) were fitted, up to 0.407 m, with Eq. (22). The values of the A-, B-, and D-coefficients calculated with the present viscosity data together with data reported by other authors at low concentrations are presented in Table VII for various temperatures. As one can see from this table the values of the D-coefficient are monotonically decreasing with temperature, which is different from the behavior of the A- and B- coefficients. The temperature dependence of the viscosity D-coefficient for K_2SO_4 (aq) is depicted in Fig. 21c together with values reported by other authors.

5. CONCLUSIONS

The thermal conductivity of three (0.239, 0.499, and 0.782 mol·kg^{-1}) and the viscosity of four (0.0658, 0.2055, 0.3050, and 0.4070 mol·kg^{-1}) binary aqueous K_2SO_4 solutions have been measured with coaxial-cylinder (steady-state) and capillary-flow techniques, respectively. Measurements were made at pressures up to 30 MPa. The range of temperature was 298 to 573 K. The total uncertainties of the thermal conductivity, viscosity, pressure, temperature, and composition measurements were estimated to be less than 2%, 1.6%, 0.05%, 30 mK, and 0.02%, respectively. The reliability and accuracy of the experimental method was confirmed with measurements on pure water. The experimental and calculated values of the thermal conductivity and viscosity for pure water from the IAPWS [54] formulation show excellent agreement within their experimental uncertainties (AAD = 0.31% and 0.52%, respectively). The measured thermal conductivity and viscosity values of solutions at atmospheric and high pressures were compared with data reported in the literature. Good agreement (within ±0.6% for the thermal conductivity and ±0.8% for the viscosity) is found between the present measurements and the data sets reported by other authors. The temperature, pressure, and concentration dependences of the thermal conductivity and viscosity are analyzed. The values of the viscosity A-, B-, and D-coefficients of the extended Jones–Dole equation for the relative viscosity (η/η_0) of aqueous K_2SO_4 solutions as a function of temperature are determined.

The quality, predictive capability, and validity of the various theoretical models for the transport properties of electrolyte solutions are tested.

ACKNOWLEDGMENT

I.M. Abdulagatov thanks the Physical and Chemical Properties Division at the National Institute of Standards and Technology for the opportunity to work as a Guest Researcher at NIST during the course of this research.

REFERENCES

1. S. Gupta and J. D. Olson, *Ind. Eng. Chem. Res.* **42**:6359 (2003).
2. T. Ishii, *Chem. Eng. Sci.* **28**:1121 (1973).
3. J. W. Mullin and C. Gaska, *Can. J. Chem. Eng.* **47**:483 (1969).
4. R. H. Stokes and R. Mills, *Viscosity of Electrolytes and Related Properties* (Pergamon, New York, 1965).
5. A. L. Horvath, *Handbook of Aqueous Electrolyte Solutions: Physical Properties, Estimation Methods and Correlation Methods* (Ellis Horwood, West Sussex, England, 1985).
6. J. Jiang and S. I. Sandler, *Ind. Eng. Chem. Res.* **42**:6267 (2003).
7. M. J. C. Esteves, J. E. de M. Cardoso, and O. E. Barcia, *Ind. Eng. Chem. Res.* **40**:5021 (2001).
8. A. Chandra and B. Bagchi, *J. Phys. Chem.* **104**:9067 (2000).
9. A. Chandra and B. Bagchi, *J. Chem. Phys.* **113**:3226 (2000).
10. B. C. Harrap and E. Heymann, *Chem. Rev.* **48**:45 (1951).
11. M. M. Lencka, A. Anderko, S. J. Sandlers, and R. D. Young, *Int. J. Thermophys.* **19**:367 (1998).
12. G. A. Vernigora, T. V. Mozharova, and E. I. Chernen'kaya, NIOKhIM Report, VNTIC #77045565, **2**:311 (1980).
13. N. B. Vargaftik and Yu. P. Os'minin, *Teploenergetika* **7**:15 (1956).
14. L. Riedel, *Chem. Ing. Tech.* **23**:59 (1951).
15. T. Barratt and H. R. Nettlrton, eds., *International Critical Tables, Thermal Conductivity of Aqueous Solutions*, (McGraw-Hill, New York, 1929), Vol. 5.
16. I. D. Zaytsev and G. G. Aseyev, *Properties of Aqueous Solutions of Electrolytes* (CRC Press, Boca Raton, Ann Arbor, London, Tokyo, 1992).
17. R. J. Correia and J. Kestin, *J. Chem. Eng. Data* **26**:43 (1981).
18. L. V. Puchkov and P. M. Sargaev, *Russ. J. Appl. Chem.* **1**:96 (1974).
19. I. N. Maksimova, J. S. Pack, and N. N. Pravdin, *Electrolyte Properties. A Handbook* (Metallurgy Press, Moscow, 1987).
20. N. A. Chesnokov, *Proc. VNII Metrology* **62**:44 (1962).
21. M. Kaminsky, *Z. Phys. Chem.* **12**:206 (1957).
22. G. Jones and J. H. Colvin, *J. Am. Chem. Soc.* **62**:338 (1940).
23. S.J. Bates and W.P. Baxter, eds., *International Critical Tables, Viscosity of Aqueous Solutions of Strong Electrolytes*, (McGraw-Hill, New York, 1928), Vol. 3, pp. 12–19.
24. W. Herz and E. Martin, *Zeit. Anorg. Chem.* **132**:41 (1924).
25. M. Tanaka, *Nippon Kagaku Zasshi* **83**:645 (1962).
26. L. L. Ezrokhi, *Russ. J. Appl. Chem.* **25**:917 (1952).

27. W. J. Sulston, *Proc. Phys. Soc. (London)* **47**:657 (1935).
28. T. Ishii and S. Fujita, *J. Chem. Eng. Data* **23**:19 (1978).
29. I. M. Abdulagatov and U. B. Magomedov, *Int. J. Thermophys.* **20**:187 (1999).
30. I. M. Abdulagatov and U. B. Magomedov, *Int. J. Thermophys*. **15**:401 (1994).
31. I. M. Abdulagatov and U. B. Magomedov, *Ind. Eng. Chem. Res.* **37**:4883 (1998).
32. I. M. Abdulagatov and U. B. Magomedov, *Ber. Bunsenges. Phys. Chem.* **101**:708 (1997).
33. I. M. Abdulagatov and U. B. Magomedov, *J. Chem. Eng. Data* **42**:1165 (1997).
34. I. M. Abdulagatov and U. B. Magomedov, *J. Chem. Eng. Japan.* **32**:465 (1999).
35. I. M. Abdulagatov and U. B. Magomedov, *High Temp.-High Press.* **32**:599 (2000).
36. I. M. Abdulagatov and U. B. Magomedov, *Fluid Phase Equilib.* **171**:243 (2000).
37. I. M. Abdulagatov and U. B. Magomedov, *High Temp.-High Press.* **35/36**:149 (2004).
38. I. M. Abdulagatov and U. B. Magomedov, *J. Sol. Chem.* **30**:223 (2001).
39. I. M. Abdulagatov and U. B. Magomedov, in *Proc. 12th Int. Conference on the Props. of Water and Steam*, H. J. White, J. V. Sengers, D. B. Neumann, and J. C. Bellows, eds. (Begell House, New York, 1995), pp. 549–557.
40. I. M. Abdulagatov, L. A. Akhmedova-Azizova, and N. D. Azizov, *J. Chem. Eng. Data* **49**:688 (2004).
41. I. M. Abdulagatov, L. A. Akhmedova-Azizova, and N. D. Azizov, *J. Chem. Eng. Data* **49**:1727 (2004).
42. N. D. Azizov, *Russ. High Temp.* **37**:649 (1999).
43. I. M. Abdulagatov and N. D. Azizov, *J. Chem. Eng. Data* **48**:1549 (2003).
44. I. M. Abdulagatov and N. D. Azizov, *J. Chem. Eng. Data* **49**:1444 (2004)
45. I. M. Abdulagatov and N. D. Azizov, *Ind. Eng. Chem. Res.* **44**:416 (2005)
46. I. M. Abdulagatov, A. Zeinalova, and N. D. Azizov, *Fluid Phase Equilib.* **227**:57 (2005)
47. N. D. Azizov and T. S. Akhundov, *Russ. J. Phys. Chem.* **71**:1955 (1997)
48. G. G. Aseyev, *Electrolytes. Properties of Solutions. Methods for Calculation of Multicomponent Systems and Experimental Data on Thermal Conductivity and Surface Tension* (Begell-House, New York, 1998)
49. U. B. Magomedov, Ph. D. Thesis, Moscow Power Engineering Institute, Moscow, 1996.
50. R. M. DiGuilio, R. J. Lee, S. M. Jeter, and A. S. Teja, *ASHRAE Trans*. **96**:702 (1990)
51. R. M. DiGuilio and A. S. Teja, *Ind. Eng. Chem. Res.* **31**:1081 (1992)
52. J. G. Bleazard, R. M. DiGuilio, and A. S. Teja, *AIChE Symp. Ser.* **298**:23 (1994)
53. J. G. Bleazard and A. S. Teja, *J. Chem. Eng. Data* **40**:732 (1995)
54. J. Kestin, J. V. Sengers, B. Kamgar-Parsi, and J. M. H. Levelt Sengers, *J. Phys. Chem. Ref. Data* **13**:175 (1984)
55. G. Z. Gershuni, *Dok. Akad. Nauk USSR* **86**:697 (1952)
56. M. L. V. Ramires, C. A. Nieto de Castro, Y. Nagasaka, A. Nagashima, M. J. Assael, and W. A. Wakeham, *J. Phys. Chem. Ref. Data* **24**:1377 (1995)
57. N. D. Azizov, *Russ. J. Inorg. Chem.* **43**:1296 (1998)
58. N. D. Azizov, *Russ. J. Inorg. Chem.* **43**:323 (1998)
59. V. D. Usufova, R. I. Pepinov, V. A. Nikolaev, and G. M. Guseinov, *Russ. J. Phys. Chem.* **49**:2677 (1975)
60. V. A. Nikolaev, Ph. D. Thesis, AzNeftChem, Baku, 1984
61. A. Chiquillo, *Measurements of the Relative Thermal Conductivity of Aqueous Salt Solutions with a Transient Hot-Wire Method* (Juris Druck+Verlag, Zurich, 1967)
62. H. Falkenhagen, *Theorie der Elektrolyte* (S. Hirzel, Leipzig, 1971)
63. H. Falkenhagen, *Z. Phys.* **32**:745 (1931)
64. M. Kaminsky, *Z. Phys. Chem.* **5**:154 (1955)
65. G. Jones and S. K. Talley, *J. Am. Chem. Soc.* **55**:4124 (1933)
66. E. Hückel and H. Schaaf, *Z. Phys. Chem. N.F.* **21**:326 (1959)

67. M. Kaminsky, *Z. Phys. Chem. (N.F.)* **8**:173 (1956)
68. R. A. Robinson and R. H. Stokes, *Electrolyte Solutions*, 2nd edn. (Butterworths, London, 1959)
69. D. J. P. Out and J. M. Los, *J. Sol. Chem.* **9**:19 (1980)
70. R. Dordick, L. Korson, and W. Drost-Hansen, *J. Coll. Inter. Sci.* **72**:206 (1979)
71. R. S. Dordick and W. Drost-Hansen, *J. Phys. Chem.* **85**:1086 (1981)
72. J. E. Desnoyers and G. Perron, *J. Sol. Chem.* **1**:199 (1972)
73. R. L. Kay, T. Vituccio, C. Zawoyski, and D. F. Evans, *J. Phys. Chem.* **70**:2336 (1966)
74. Y. C. Wu, *J. Phys. Chem.* **72**:2663 (1968)
75. R. A. Horne, ed., *Water and Aqueous Solutions, Structure, Thermodynamics, and Transport Properties.* (Wiley Interscience, New York, 1972)
76. H. D. B. Jenkins and Y. Marcus, *Chem. Rev.* **95**:2695 (1995)
77. W. M. Cox and J. H. Wolfenden, *Proc. R. Soc. A. (London)* **145**:475 (1934)
78. L. Onsager and R. M. Fuoss, *J. Phys. Chem.* **36**:2689 (1932)
79. H. Falkenhagen and M. Dole, *Phys. Z.* **30**:611 (1929)
80. P. Debye and H. Hückel, *Z. Phys.* **25**:49 (1924)
81. L. Onsager, *Z. Phys.* **27**:388 (1926)
82. G. Jones and M. Dole, *J. Am. Chem. Soc.* **51**:2950 (1929)
83. H. S. Frank and W. Y. Wen, *Discuss. Faraday Soc.* **24**:133 (1957)
84. M. Kaminsky, *Discuss. Faraday Soc.* **24**:171 (1957)
85. F. J. Millero, W. Drost-Hansen, and L. Korson, *J. Phys. Chem.* **72**:2251 (1968)
86. I. M. Abdulagatov and N. D. Azizov, *J. Chem. Thermodyn.* **36**:17 (2004)
87. I. M. Abdulagatov and N. D. Azizov, *Int. J. Thermophys.* **24**:1581 (2003)
88. I. M. Abdulagatov and N. D. Azizov, *J. Sol. Chem.*, **32**:573 (2003)
89. I. M. Abdulagatov and N. D. Azizov, *High Temp.-High Press.* (in press)
90. I. M. Abdulagatov and N. D. Azizov, *J. Sol. Chem.* **33**:1305 (2004)
91. L. Hnědkovský, V. Majer, and R. H. Wood, *J. Chem. Thermodyn.* **27**:801 (1995)
92. J. G. Ganopolsky, H. L. Bianchi, and H. R. Corti, *J. Sol. Chem.* **27**:377 (1995)
93. M. Obšil, V. Majer, G. T. Hefter, and V. Hynek, *J. Chem. Thermodyn.* **42**:137 (1997)
94. V. Majer, A. Inglese, and R. H. Wood, *J. Chem. Thermodyn.* **21**:321 (1989)
95. A. Einstein, *Ann. Phys.* **34**:591 (1911)
96. J. Happel, *J. App. Phys.* **28**:1288 (1957)
97. J. F. Skinner and R. M. Fuoss, *J. Phys. Chem.* **67**:2998 (1964)
98. D. G. Thomas, *J. Colloid Sci.* **20**:267 (1965)
99. B. R. Breslau and I. F. Millero, *J. Phys. Chem.* **74**:1056 (1970)
100. S. P. Moulik and A. K. Rakshit, *J. Ind. Chem. Soc.* **52**:450 (1975)
101. D. Feakins and D. G. Lawrence, *Chem. Soc. A.* **212**:(1966)
102. J. E. Desnoyers, M. Arel, and P. A. Leduc, *Can. J. Chem.* **47**:547 (1969)
103. C. T. Robertson and H. J. U. Tyrrell, *J. Chem. Soc. A.* 1938 (1969)
104. N. V. Lobkova and R. I. Pepinov, *Russ. J. Phys. Chem.* **53**:1765 (1979).